**Acknowledgments**

We thank R Benezra, S Choe, NG Copeland, R Eckner, D Melton, K Miyazono, G Tiscornia, and S Yamanaka for reagents; D Buscher, C Kintner, I Oishi, J Sonoda, and A Tashiro for helpful suggestions; H Pineda, T Chapman, and H Juguilon for technical assistance; and M-F Schwarz for help with this manuscript. AS, TM, and KN received support from the Japan Society for the Promotion of Science, and AR and CR-E from the Fundación Inbiomed, Spain. We are also indebted for support to the Salk Institute, the Lookout Fund, the G Harold and Leila Y Mathers Charitable Foundation, and the National Institutes of Health.

**Competing interests**

The authors declared they have no competing interests.

fates (Figure 4). The requirement of LIF/STAT3 signaling for the maintenance of mouse ESCs has been related to the ability of preimplantation mouse embryos to arrest development when implantation is prevented (a phenomenon known as dispause[25]). In keeping with this idea, it appears reasonable that cells in the inner cell mass of mouse blastocysts evolve specific mechanisms to prevent unwanted cell differentiation during dispause. The mechanism described in this study could very well serve this purpose. In contrast, ESCs derived from human embryos, in which dispause does not occur, do not depend on LIF/STAT3 signaling to maintain pluripotency.[26] Interestingly, the Nanog-mediated negative feedback mechanism characterized in this study does not appear to be operative in human ESCs, since, unlike mouse ESCs, human ESCs do not upregulate *Nanog* expression in response to LIF and bone morphogenetic protein stimulation, even though *T* expression is induced under these conditions (unpublished data). The absence of a functional negative feedback mechanism mediated by T, LIF/STAT3, and Nanog in human ESCs provides additional mechanistic insights into the reasons why LIF is dispensable for the self-renewal of human ESCs.

## CONCLUSION

Taken together, our results uncover a mechanism underlying mouse ESC pluripotency, by which specified mesoderm progenitors undergo an active process of dedifferentiation mediated by the combined action of the extrinsic cytokine LIF and the intrinsic pluripotency factor Nanog. These findings contribute to unraveling the complex network of molecular interactions required to maintain the self-renewal of ESCs and shed light on the cellular bases of ESC pluripotency. Furthermore, the possibility of reverting the differentiation status of specified or committed cells offers new ways to approach the generation of pluripotent cells for future therapeutic interventions of regenerative medicine.

**References**

1 Martin GR (1981) Isolation of a pluripotent cell line from early mouse embryos cultured in medium conditioned by teratocarcinoma stem cells. *Proc Natl Acad Sci USA* **78:** 7634–7638
2 Evans MJ and Kaufman MH (1981) Establishment in culture of pluripotential cells from mouse embryos. *Nature* **292:** 154–156
3 Smith AG (2001) Embryo-derived stem cells: of mice and men. *Annu Rev Cell Dev Biol* **17:** 435–462
4 Shamblott MJ *et al.* (1998) Derivation of pluripotent stem cells from cultured human primordial germ cells. *Proc Natl Acad Sci USA* **95:** 13726–13731
5 Thomson JA *et al.* (1998) Embryonic stem cell lines derived from human blastocysts. *Science* **282:** 1145–1147
6 Rao M (2004) Conserved and divergent paths that regulate self-renewal in mouse and human embryonic stem cells. *Dev Biol* **275:** 269–286
7 Herrmann BG *et al.* (1990) Cloning of the T gene required in mesoderm formation in the mouse. *Nature* **343:** 617–622
8 Wilkinson DG *et al.* (1990) Expression pattern of the mouse T gene and its role in mesoderm formation. *Nature* **343:** 657–659
9 Smith AG *et al.* (1988) Inhibition of pluripotential embryonic stem cell differentiation by purified polypeptides. *Nature* **336:** 688–690
10 Williams RL *et al.* (1988) Myeloid leukaemia inhibitory factor maintains the developmental potential of embryonic stem cells. *Nature* **336:** 684–687
11 Mitsui K *et al.* (2003) The homeoprotein Nanog is required for maintenance of pluripotency in mouse epiblast and ES cells. *Cell* **113:** 631–642
12 Chambers I *et al.* (2003) Functional expression cloning of Nanog, a pluripotency sustaining factor in embryonic stem cells. *Cell* **113:** 643–655
13 Li E *et al.* (1992) Targeted mutation of the DNA methyltransferase gene results in embryonic lethality. *Cell* **69:** 915–926
14 Cowan CA *et al.* (2004) Derivation of embryonic stem-cell lines from human blastocysts. *N Engl J Med* **350:** 1353–1356
15 Yu D *et al.* (2000) An efficient recombination system for chromosome engineering in *Escherichia coli*. *Proc Natl Acad Sci USA* **97:** 5978–5983
16 Suzuki A *et al.* (2000) Flow-cytometric separation and enrichment of hepatic progenitor cells in the developing mouse liver. *Hepatology* **32:** 1230–1239
17 Suzuki A *et al.* (2003) Role for growth factors and extracellular matrix in controlling differentiation of prospectively isolated hepatic stem cells. *Development* **130:** 2513–2524
18 Ramalho-Santos M *et al.* (2002) "Stemness": transcriptional profiling of embryonic and adult stem cells. *Science* **298:** 597–600
19 Raz R *et al.* (1999) Essential role of STAT3 for embryonic stem cell pluripotency. *Proc Natl Acad Sci USA* **96:** 2846–2851
20 Gossen M *et al.* (1995) Transcriptional activation by tetracyclines in mammalian cells. *Science* **268:** 1766–1769
21 Hoffmann A *et al.* (2002) The T-box transcription factor Brachyury mediates cartilage development in mesenchymal stem cell line C3H10T1/2. *J Cell Sci* **115:** 769–781
22 Rashbass P *et al.* (1991) A cell autonomous function of Brachyury in T/T embryonic stem cell chimaeras. *Nature* **353:** 348–351
23 Kubo A *et al.* (2004) Development of definitive endoderm from embryonic stem cells in culture. *Development* **131:** 1651–1662
24 Rathjen J *et al.* (1999) Formation of a primitive ectoderm like cell population, EPL cells, from ES cells in response to biologically derived factors. *J Cell Sci* **112 ( Pt 5):** 601–612
25 Nichols J *et al.* (2001) Physiological rationale for responsiveness of mouse embryonic stem cells to gp130 cytokines. *Development* **128:** 2333–2339
26 Daheron L *et al.* (2004) LIF/STAT3 signaling fails to maintain self-renewal of human embryonic stem cells. *Stem Cells* **22:** 770–778

PNAS
Proceedings of the National Academy of Sciences of the United States of America www.pnas.org

# Nanog binds to Smad1 and blocks bone morphogenetic protein-induced differentiation of embryonic stem cells

Atsushi Suzuki, Ángel Raya, Yasuhiko Kawakami, Masanobu Morita, Takaaki Matsui, Kinichi Nakashima, Fred H. Gage, Concepción Rodríguez-Esteban, and Juan Carlos Izpisúa Belmonte

*PNAS* 2006;103;10294-10299; originally published online Jun 26, 2006;
doi:10.1073/pnas.0506945103

# TLR-Dependent Induction of IFN-β Mediates Host Defense against *Trypanosoma cruzi*[1]

**Ritsuko Koga,* Shinjiro Hamano,† Hirotaka Kuwata,* Koji Atarashi,* Masahiro Ogawa,* Hajime Hisaeda,† Masahiro Yamamoto,‡ Shizuo Akira,‡ Kunisuke Himeno,† Makoto Matsumoto,* and Kiyoshi Takeda[2]***

**Host resistance to the intracellular protozoan parasite *Trypanosoma cruzi* depends on IFN-γ production by T cells and NK cells. However, the involvement of innate immunity in host resistance to *T. cruzi* remains unclear. In the present study, we investigated host defense against *T. cruzi* by focusing on innate immunity. Macrophages and dendritic cells (DCs) from MyD88$^{-/-}$TRIF$^{-/-}$ mice, in which TLR-dependent activation of innate immunity was abolished, were defective in the clearance of *T. cruzi* and showed impaired induction of IFN-β during *T. cruzi* infection. Neutralization of IFN-β in MyD88$^{-/-}$ macrophages led to enhanced *T. cruzi* growth. Cells from MyD88$^{-/-}$IFNAR1$^{-/-}$ mice also showed impaired *T. cruzi* clearance. Furthermore, both MyD88$^{-/-}$TRIF$^{-/-}$ and MyD88$^{-/-}$IFNAR1$^{-/-}$ mice were highly susceptible to in vivo *T. cruzi* infection, highlighting the involvement of innate immune responses in *T. cruzi* infection. We further analyzed the molecular mechanisms for the IFN-β-mediated antitrypanosomal innate immune responses. MyD88$^{-/-}$TRIF$^{-/-}$ and MyD88$^{-/-}$IFNAR1$^{-/-}$ macrophages and DCs exhibited defective induction of the GTPase IFN-inducible p47 (IRG47) after *T. cruzi* infection. RNA interference-mediated reduction of IRG47 expression in MyD88$^{-/-}$ macrophages resulted in increased intracellular growth of *T. cruzi*. These findings suggest that TLR-dependent expression of IFN-β is involved in resistance to *T. cruzi* infection through the induction of IRG47. *The Journal of Immunology*, 2006, 177: 7059–7066.**

The parasite *Trypanosoma cruzi* is an intracellular protozoan that causes Chagas' disease, a chronic systemic disorder affecting nearly 20 million people in Central and South America. Host defense against *T. cruzi* depends on a variety of cell populations, including NK, CD4$^+$ T cells, CD8$^+$ T cells, and Ig-producing B cells (1–3). In addition, macrophages and dendritic cells (DCs)[3] produce proinflammatory cytokines, such as IL-12, in response to invasion by *T. cruzi* (4–6). IL-12 induces IFN-γ production by NK, CD4$^+$ T cells, and CD8$^+$ T cells. In turn, IFN-γ induces NO production by macrophages and mediates the killing of *T. cruzi* (7, 8). This cytokine milieu is therefore responsible for host resistance to *T. cruzi* infection in vivo. However, it remains uncertain how innate immune cells, such as macrophages and DCs, mediate *T. cruzi*-induced immune responses during the early phase of infection. In addition, *T. cruzi* infection induces the production of type I IFNs (αβ IFN), which possess antiviral activities (9, 10). However, the nature of the involvement of type I IFNs in response to *T. cruzi* infection remains controversial (11).

A family of TLRs has been identified that recognize specific components of various microorganisms, including bacteria, viruses, fungi, and protozoan parasites (12). Recognition of microbial components by TLRs triggers the activation of innate immunity and the subsequent development of Ag-specific adaptive immunity. TLR-mediated signaling pathways originate from the cytoplasmic Toll/IL-1R (TIR) domains, which are conserved among all family members. A group of TIR domain-containing adaptors (MyD88, Toll/IL-1R domain-containing adaptor protein, TIR domain-containing adaptor-inducing IFN-β (TRIF), and TRIF-related adaptor molecule) have been shown to be integral to these TLR signaling pathways (13). The TLR signaling pathways consist of two cascades: a MyD88-dependent pathway and a TRIF-dependent (MyD88-independent) pathway. The MyD88-dependent pathway mediates all TLR-induced productions of proinflammatory cytokines, including IL-12p40, whereas the TRIF-dependent pathway is indispensable for the induction of type I IFNs through TLR3 and TLR4.

Previous studies have analyzed the involvement of TLR-dependent activation of innate immunity in *T. cruzi* infection. TLR2, TLR4, and TLR9 have been implicated in the recognition of *T. cruzi*-derived components (6, 14–16), whereas mice lacking MyD88 were found to be susceptible to the acute phase of *T. cruzi* infection accompanied by defective proinflammatory cytokine production (17). However, even in MyD88-deficient mice, significant IFN-γ production was still observed, indicating the presence of MyD88-independent immune responses. Thus, the nature of the involvement of innate immunity in *T. cruzi* infection still remains to be precisely characterized.

In the present study, we analyzed the involvement of innate immune cells in *T. cruzi* infection using mice lacking both

*Department of Molecular Genetics, Medical Institute of Bioregulation and †Department of Parasitology, Faculty of Medical Sciences, Kyushu University, Fukuoka, Japan; and ‡Department of Host Defense, Institute for Microbial Diseases, Osaka University, and Exploratory Research for Advanced Technology, Japan Science and Technology Agency, Suita, Japan

Received for publication May 31, 2006. Accepted for publication September 1, 2006.

The costs of publication of this article were defrayed in part by the payment of page charges. This article must therefore be hereby marked *advertisement* in accordance with 18 U.S.C. Section 1734 solely to indicate this fact.

[1] This work was supported by grants from the Special Coordination Funds of the Ministry of Education, Culture, Sports, Science and Technology, as well as the Uehara Memorial Foundation, the Mitsubishi Foundation, the Takeda Science Foundation, the Tokyo Biochemical Research Foundation, the Kowa Life Science Foundation, the Osaka Foundation for Promotion of Clinical Immunology, and the Sankyo Foundation of Life Science.

[2] Address correspondence and reprint requests to Dr. Kiyoshi Takeda, Department of Molecular Genetics, Medical Institute of Bioregulation, Kyushu University, 3-1-1 Maidashi, Higashi-ku, Fukuoka 812-8582, Japan. E-mail address: ktakeda@bioreg.kyushu-u.ac.jp

[3] Abbreviations used in this paper: DC, dendritic cell; TIR, Toll/IL-1R; TRIF, TIR domain-containing adaptor-inducing IFN-β; WT, wild type; siRNA, small interfering RNA; EF-1α, elongation factor-1α.



0022-1767/06/$02.00

MyD88 and TRIF, in which all of the previously described TLR-mediated activation mechanisms of innate immunity are totally abolished.

## Materials and Methods

### *Mice*

MyD88$^{-/-}$ and TRIF$^{-/-}$ mice were generated as previously described (18, 19). Type I IFN receptor (IFNAR1)$^{-/-}$ mice were purchased from B & K Universal (20). Each mouse strain was backcrossed to C57BL/6 for at least five generations, and then used to generate double-mutant mice. MyD88$^{-/-}$TRIF$^{-/-}$ mice were generated by crossing MyD88$^{+/-}$ TRIF$^{+/-}$ mice. Littermate wild-type (WT) (MyD88$^{+/-}$TRIF$^{+/-}$), MyD88$^{-/-}$ (MyD88$^{-/-}$TRIF$^{+/-}$), and TRIF$^{-/-}$ (MyD88$^{+/-}$TRIF$^{-/-}$) mice were used for the experiments. MyD88$^{-/-}$IFNAR1$^{-/-}$ mice were generated by crossing MyD88$^{+/-}$IFNAR1$^{+/-}$ mice, and used for the experiments at 8–10 wk of age. All animal experiments were conducted in accordance with the guidelines of the Animal Care and Use Committee of Kyushu University.

### *Preparation of macrophages and DCs*

To isolate peritoneal macrophages, mice were i.p. injected with 2 ml of 4% thioglycolate medium (Sigma-Aldrich), and peritoneal exudate cells were isolated from the peritoneal cavity at 3 days postinjection. The cells were incubated for 2 h and washed three times with HBSS. The remaining adherent cells were used as peritoneal macrophages in experiments. To prepare bone marrow-derived DCs or macrophages, bone marrow cells were prepared from the femur and tibia, passed through a nylon mesh and cultured in RPMI 1640 medium supplemented with 10% FBS, 100 mM 2-ME, and 10 ng/ml GM-CSF (PeproTech) or 30% L cell culture supernatant. After 6 days, the cells were used as DCs or macrophages in experiments.

### *Parasites and experimental infection*

The *T. cruzi* Tulahuén strain was maintained in vivo in IFN-γR$^{-/-}$ mice by passages every other week (21). For in vitro experiments, macrophages or DCs ($5 \times 10^4$) were infected with $5 \times 10^4$ trypomastigotes. After 6 h of infection, the cells were washed twice with PBS to remove the extracellular parasites and cultured in RPMI 1640 supplemented with 10% FBS for the indicated time periods. Trypomastigotes in the culture supernatants were counted microscopically. Alternatively, the cells were pulsed with 1 μCi of [$^3$H]uracil and cultured for 72 h. The cells were then harvested on glass fiber filters and the incorporated uracil was measured using a liquid scintillation counter. The net cpm was calculated by subtracting the background cpm in uninfected cultures from the cpm of the infected cultures. In some experiments, macrophages were infected with *T. cruzi* in the absence or presence of 10 ng/ml of an anti-IFN-β neutralizing Ab (YAMASA) for 6 h, washed and then further cultured with or without the anti-IFN-β Ab.

In other experiments, extracellular parasites were removed by repeated washing after 6h of infection, and the cells were incubated for a further 48 h. Subsequently, the cells were washed, fixed and stained using a Diff-Quik kit (Sysmex). The intracellular parasite numbers in 250 macrophages were counted under a light microscope. Counting was performed in a blinded manner by two independent investigators.

For in vivo experiments, mice were i.p. injected with plasma containing $2 \times 10^3$ or $1 \times 10^4$ trypomastigotes as indicated. The number of parasites in the blood of each animal was then counted microscopically using 5 μl of blood taken from the tail. Statistical significance was determined using a paired Student's *t* test. Differences were considered to be statistically significant at $p < 0.05$.

### *Measurement of cytokine production*

Peritoneal macrophages or DCs ($5 \times 10^4$) were infected with $5 \times 10^4$ *T. cruzi* for 6 h, extensively washed and cultured for 24 h. The culture supernatants were collected and analyzed for their levels of TNF-α by ELISA (Genzyme Techne) and NO using the Griess reagent (Dojindo Laboratories).

### *Quantitative real-time RT-PCR*

Total RNA was isolated with an RNeasy mini kit (Qiagen), and 2 μg of the RNA was reverse-transcribed using M-MLV reverse transcriptase (Promega) and oligo(dT) primers (Toyobo) after treatment with RQ1 DNase I (Promega). Quantitative real-time PCR was performed in an ABI 7000 (Applied Biosystems) using TaqMan Universal PCR Master Mix (Applied Biosystems). All data were normalized to the corresponding level of elongation factor-1α (EF-1α) expression, and the fold difference relative to the EF-1α level was calculated. The amplification conditions were: 50°C (2 min), 95°C (10 min), and 40 cycles of 95°C (15 s), and 60°C (60 s). Each experiment was performed independently at least three times, and the results of one representative experiment are shown. All primers were purchased from Assay on Demand (Applied Biosystems).

### *RNA interference*

For small interfering RNA (siRNA) experiments, dsRNA duplexes targeting the coding region of the GTPase IFN-inducible p47 (IRG47) (5′-GGUGGAUAGUGACUUAUAUtt-3′) were synthesized by Ambion. Bone marrow cells were cultured in the presence of 30% L cell culture supernatant for 6 days. The differentiated bone marrow macrophages were then harvested by 5 mM EDTA treatment and transfected with 1.5 μg of the siRNA using Nucleofector and a Mouse Macrophage Nucleofector kit (Amaxa Biosystems) according to the manufacturer's instructions. The cells were immediately transferred to culture medium and cultured for 18 h. Next, cells were infected with *T. cruzi* for 48 h, and parasite growth was analyzed. To determine the efficiency of gene silencing, cells were infected with *T. cruzi* for 6 h, and the expression of IRG47 mRNA was analyzed by quantitative real-time RT-PCR.

## Results

### *Increased growth of* T. cruzi *in MyD88$^{-/-}$TRIF$^{-/-}$ DCs and macrophages*

To study the direct involvement of innate immunity in *T. cruzi* infection, bone marrow-derived DCs prepared from WT, MyD88$^{-/-}$, TRIF$^{-/-}$, or MyD88$^{-/-}$TRIF$^{-/-}$ mice were infected with *T. cruzi*. After 6 h of *T. cruzi* infection, the cells were extensively washed and changed to fresh medium. After culture periods of 4, 5, and 7 days, the number of trypomastigotes released into the culture supernatants were counted (Fig. 1*A*). The culture supernatant of TRIF$^{-/-}$ DCs contained a similar number of trypomastigotes to that of WT DCs. For MyD88$^{-/-}$ DCs, the number of trypomastigotes increased after 5 and 7 days of infection. Furthermore, for MyD88$^{-/-}$TRIF$^{-/-}$ DCs, the number of trypomastigotes increased considerably. Next, peritoneal macrophages were infected with *T. cruzi* (Fig. 1*B*). The number of trypomastigotes in the culture supernatant of MyD88$^{-/-}$ macrophages was slightly increased compared with those of WT or TRIF$^{-/-}$ cells after 5 and 7 days of infection. For MyD88$^{-/-}$TRIF$^{-/-}$ macrophages, larger numbers of trypomastigotes were observed compared with the other cell genotypes after 7 days of infection. Next, replication of *T. cruzi* within macrophages was assessed based on [$^3$H]uracil incorporation (Fig. 1*C*). Intracellular growth of *T. cruzi* was slightly increased in MyD88$^{-/-}$ macrophages, and markedly increased in MyD88$^{-/-}$TRIF$^{-/-}$ cells compared with WT cells. Bone marrow-derived macrophages were also infected with *T. cruzi* and cultured for 48 h, before the number of intracellular parasites was counted. The number of infected cells did not differ among the genotypes (data not shown). However, infected MyD88$^{-/-}$TRIF$^{-/-}$ macrophages contained an increased number of parasites after 48 h of infection (Fig. 1, *D* and *E*). Thus MyD88$^{-/-}$ DCs and macrophages showed a slight increase in *T. cruzi* growth, whereas MyD88$^{-/-}$TRIF$^{-/-}$ cells showed a marked increase in growth, indicating that MyD88$^{-/-}$TRIF$^{-/-}$ DCs and macrophages were defective in the clearance of *T. cruzi*.

### *Defective* T. cruzi *induction of proinflammatory mediators in MyD88$^{-/-}$ macrophages and DCs*

The killing of parasites by macrophages has been shown to be mediated by TNF-α and NO (22–25). Therefore, we next analyzed the production of TNF-α and NO by *T. cruzi*-infected peritoneal macrophages (Fig. 2). Both WT and TRIF$^{-/-}$ macrophages secreted TNF-α and NO in response to *T. cruzi* infection. In contrast,

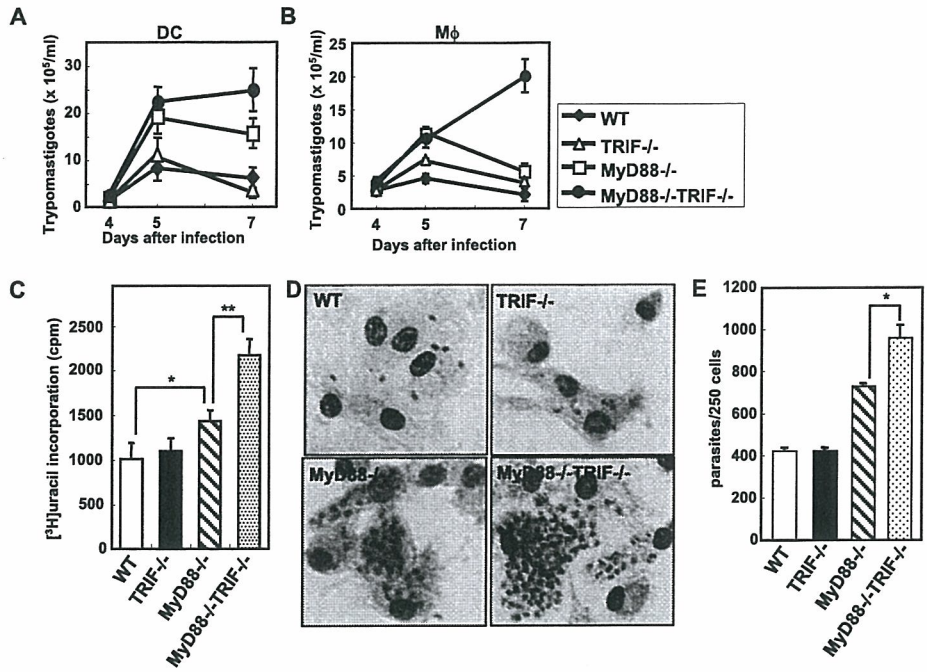


**FIGURE 1.** Defective *T. cruzi* clearance in MyD88$^{-/-}$TRIF$^{-/-}$ DCs and macrophages. Bone marrow-derived DCs (*A*) or peritoneal macrophages (M$\phi$) (*B*) from WT, TRIF$^{-/-}$, MyD88$^{-/-}$, or MyD88$^{-/-}$TRIF$^{-/-}$ mice were seeded onto 96-well plates, and infected with *T. cruzi* for 6 h. The cells were then washed to remove the extracellular parasites and cultured for the indicated periods, before the numbers of trypomastigotes in the culture supernatants were counted. Data are representative of four independent experiments. *C*, Peritoneal macrophages were infected with *T. cruzi*, washed and cultured in the presence of [$^3$H]uracil for 72 h, before the [$^3$H]uracil incorporation was measured. *, $p < 0.01$; **, $p < 0.005$. *D* and *E*, Bone marrow-derived macrophages were infected with *T. cruzi*, washed, and cultured for 48 h. The cells were then fixed, stained, and analyzed by microscopy. Representative stained cells from three independent experiments are shown. Magnification, ×400. The intracellular parasites were counted, and the data represent the mean + SD of the number of parasites per 250 macrophages. *, $p < 0.02$.

secretion of these mediators was severely reduced in both MyD88$^{-/-}$ and MyD88$^{-/-}$TRIF$^{-/-}$ macrophages, and no significant differences were observed between the two genotypes. These findings indicate that *T. cruzi*-induced production of TNF-$\alpha$ and NO was dependent on MyD88, but that the higher susceptibility to *T. cruzi* infection of MyD88$^{-/-}$TRIF$^{-/-}$ macrophages was not due to defective induction of these mediators.

### *Defective* T. cruzi *induction of IFN-inducible genes in MyD88$^{-/-}$TRIF$^{-/-}$ macrophages and DCs*

Next, we tried to identify which genes were selectively less active in *T. cruzi*-infected MyD88$^{-/-}$TRIF$^{-/-}$ DCs. *T. cruzi* infection has been shown to induce IFN-$\beta$ (9, 10). Therefore, we analyzed *T. cruzi*-induced gene expression focusing on IFN-$\beta$ and IFN-inducible chemokines as well as proinflammatory cytokines in peritoneal macrophages and DCs from WT, TRIF$^{-/-}$, MyD88$^{-/-}$, and MyD88$^{-/-}$TRIF$^{-/-}$ mice by quantitative real-time RT-PCR. In WT and TRIF$^{-/-}$ macrophages, *T. cruzi* infection led to robust induction of TNF-$\alpha$ and IL-12p40 mRNAs (Fig. 3*A*). In contrast, both MyD88$^{-/-}$ and MyD88$^{-/-}$TRIF$^{-/-}$ macrophages showed defective induction of TNF-$\alpha$ and IL-12p40. Expression of the mRNAs for IFN-$\beta$ and IFN-inducible genes, such as *Ccl2* (MCP-1), *Ccl5* (RANTES), and *Cxcl10* (IP-10) was induced in *T. cruzi*-infected WT DCs (Fig. 3*B*). In contrast, *T. cruzi*-induced expression of IFN-$\alpha$4 mRNA was not observed in any of the macrophage and DC genotypes (data not shown). In MyD88$^{-/-}$ DCs, *T. cruzi*-induced expression of *Ccl2*, *Ccl5*, and *Cxcl10* was only slightly reduced. However, DCs from TRIF$^{-/-}$ and MyD88$^{-/-}$TRIF$^{-/-}$ mice showed severely impaired induction of these genes after *T. cruzi* infection. Peritoneal macrophages from each genotype showed similar patterns of *T. cruzi*-induced gene expression (Fig. 3*C*). Thus, MyD88$^{-/-}$ macrophages and DCs showed defective induction of proinflammatory cytokine genes during *T. cruzi* infection, whereas TRIF$^{-/-}$ cells showed defective induction of IFN-$\beta$ and IFN-inducible genes during the infection. Furthermore, MyD88$^{-/-}$TRIF$^{-/-}$ cells displayed defective expression of all these genes.

### *IFN-$\beta$-mediated inhibition of* T. cruzi *growth in MyD88$^{-/-}$ macrophages*

MyD88$^{-/-}$TRIF$^{-/-}$ macrophages and DCs displayed defective clearance of *T. cruzi* with impaired expression of IFN-$\beta$ and IFN-inducible genes. Therefore, we next addressed whether IFN-$\beta$ is involved in the resistance to *T. cruzi* infection in MyD88$^{-/-}$ macrophages. Peritoneal macrophages from WT and MyD88$^{-/-}$ mice were infected with *T. cruzi* in the presence of an anti-IFN-$\beta$ neutralizing Ab, and intracellular growth of *T. cruzi* was measured (Fig. 4). In WT macrophages, *T. cruzi* growth remained unaltered by the addition of the anti-IFN-$\beta$ Ab. In contrast, anti-IFN-$\beta$ Ab addition dramatically increased the intracellular growth of *T. cruzi* in MyD88$^{-/-}$ macrophages. These findings indicate the possible involvement of IFN-$\beta$ in resistance to *T. cruzi* infection in the absence of MyD88.

### *High-sensitivity to* T. cruzi *infection in MyD88$^{-/-}$IFNAR1$^{-/-}$ macrophages*

To further address whether IFN-$\beta$ is involved in the resistance to *T. cruzi* infection, we generated mice lacking both MyD88 and the IFNAR1 subunit of the $\alpha\beta$ IFN receptor complex (MyD88$^{-/-}$ IFNAR1$^{-/-}$ mice). Bone marrow-derived macrophages were infected with *T. cruzi*, washed, and cultured. After culture periods of 4, 5, and 7 days, the numbers of trypomastigotes in the culture

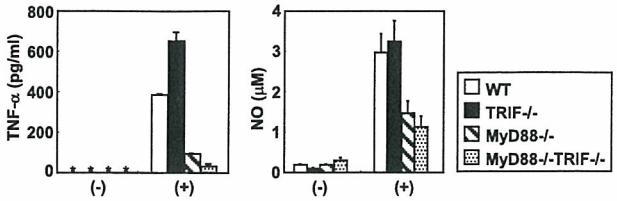


**FIGURE 2.** Defective production of TNF-α and NO in *T. cruzi*-infected MyD88$^{-/-}$ macrophages. Peritoneal macrophages from WT, TRIF$^{-/-}$, MyD88$^{-/-}$, or MyD88$^{-/-}$TRIF$^{-/-}$ mice were infected with (+) or without (−) *T. cruzi* for 6 h, washed to remove the extracellular parasites, and cultured for 24 h. The levels of TNF-α and NO in the culture supernatants were measured. *, Not detected.

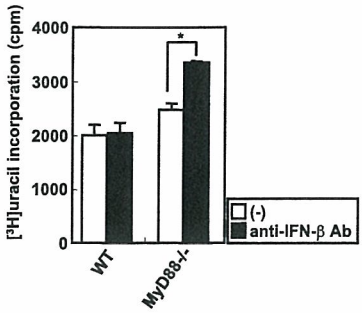


**FIGURE 4.** Effect of an anti-IFN-β neutralizing Ab on *T. cruzi* growth in macrophages. Peritoneal macrophages from WT or MyD88$^{-/-}$ mice were infected with *T. cruzi* for 6 h in the presence or absence of an anti-IFN-β neutralizing Ab, washed, and cultured in the presence of [$^3$H]uracil for 72 h. The [$^3$H]uracil incorporation was then measured. *, $p < 0.005$.

supernatants were counted (Fig. 5*A*). As mentioned, the culture supernatant of MyD88$^{-/-}$ macrophages contained a larger number of trypomastigotes than that of WT macrophages. In the supernatant of IFNAR1$^{-/-}$ macrophages, a slight increase in the number of trypomastigotes was observed compared with WT cells. Furthermore, the number of trypomastigotes in the culture supernatant of MyD88$^{-/-}$IFNAR1$^{-/-}$ macrophages was considerably increased. Next, intracellular replication of *T. cruzi* was assessed by counting [$^3$H]uracil incorporation (Fig. 5*B*). MyD88$^{-/-}$ and IFNAR1$^{-/-}$ macrophages showed slightly increased growth rates of *T. cruzi*. However, MyD88$^{-/-}$IFNAR1$^{-/-}$ macrophages showed markedly increased growth rates of *T. cruzi* compared with MyD88$^{-/-}$ or IFNAR1$^{-/-}$ cells. Furthermore, at 48 h after the *T. cruzi* infection, increased numbers of parasites were observed in MyD88$^{-/-}$IFNAR1$^{-/-}$ macrophages (Fig. 5, *C* and *D*). Thus, IFNAR1$^{-/-}$ macrophages displayed a slightly increased sensitivity to *T. cruzi* infection, whereas MyD88$^{-/-}$IFNAR1$^{-/-}$ macrophages displayed a higher sensitivity to the infection. These findings suggest that IFN-β is responsible for resistance to *T. cruzi* infection and that this responsibility becomes evident in the absence of MyD88.

### *High-sensitivity MyD88$^{-/-}$IFNAR1$^{-/-}$ mice to* T. cruzi *infection*

Macrophages are the primary site of *T. cruzi* replication, and thus act as the major cell population for controlling the infection in vivo, especially for reticulotropic strains such as the Tulahuén strain used in the present study (21, 26). Therefore, we next addressed whether IFN-β mediates antitrypanosomal responses in vivo. Mice were i.p. infected with *T. cruzi*, and the parasitemia was monitored (Fig. 6*A*). In WT and TRIF$^{-/-}$ mice, the trypomastigote counts in the sera peaked by day 13 of the infection, and subsequently decreased. In IFNAR1$^{-/-}$ mice, serum trypomastigotes were slightly increased compared with WT or TRIF$^{-/-}$ mice, and peaked around 11–13 days of infection. In MyD88$^{-/-}$ mice, the parasite counts were increased at 13 days of infection. In MyD88$^{-/-}$TRIF$^{-/-}$ mice, the serum parasite counts continued to increase, and these mice showed much higher levels of parasitemia by day 15 of infection than levels found in MyD88$^{-/-}$ mice. In MyD88$^{-/-}$IFNAR1$^{-/-}$ mice, the parasite counts increased in a similar manner

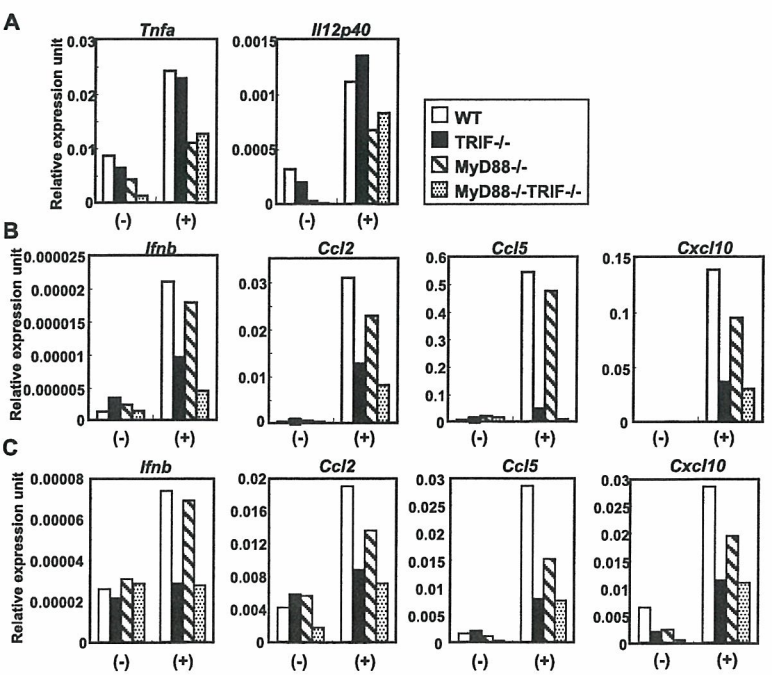


**FIGURE 3.** *T. cruzi*-induced expression of inflammatory genes in macrophages and DCs. *A*, Peritoneal macrophages from WT, TRIF$^{-/-}$, MyD88$^{-/-}$, or MyD88$^{-/-}$TRIF$^{-/-}$ mice were cultured in the presence (+) or absence (−) of *T. cruzi* for 6 h. Total RNA was then extracted and analyzed for the expressions of *Tnfa* or *Il-12p40* by quantitative real-time RT-PCR. The data are shown as the relative mRNA levels normalized by the corresponding EF-1α mRNA level. Bone marrow-derived DCs (*B*) or peritoneal macrophages (*C*) from WT, TRIF$^{-/-}$, MyD88$^{-/-}$, or MyD88$^{-/-}$TRIF$^{-/-}$ mice were cultured in the presence (+) or absence (−) of *T. cruzi* for 6 h. Total RNA was then extracted and analyzed for the expressions of *Ifnb*, *Ccl2*, *Ccl5*, and *Cxcl10* by quantitative real-time RT-PCR. Data are presented in relative expression units and have been normalized to the corresponding EF-1α mRNA level.

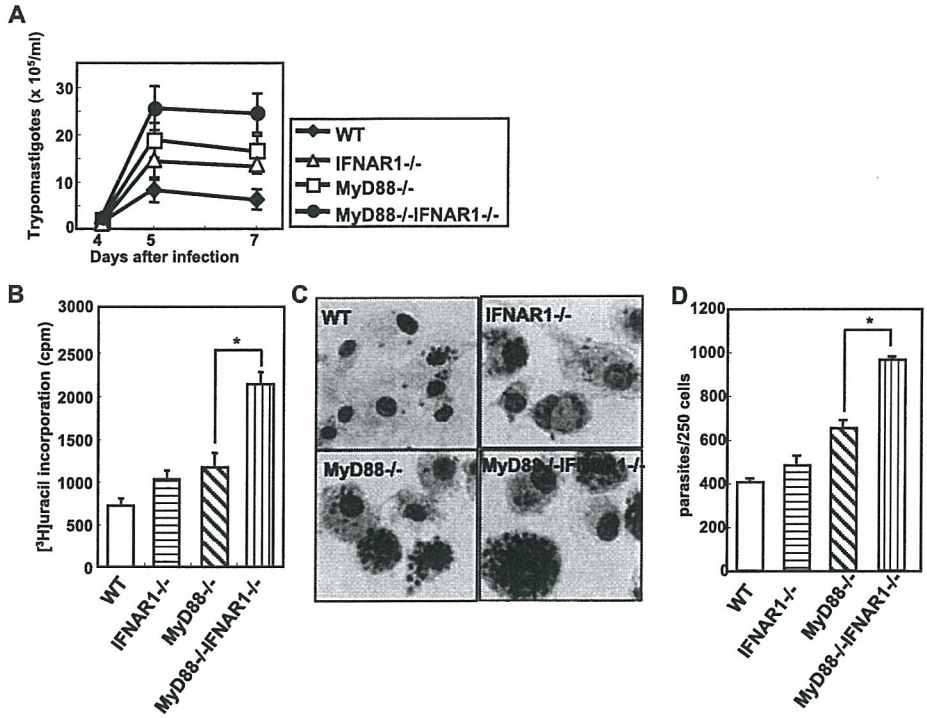


**FIGURE 5.** Increased *T. cruzi* growth in MyD88$^{-/-}$IFNAR1$^{-/-}$ macrophages. *A*, Bone marrow-derived macrophages from WT, MyD88$^{-/-}$, IFNAR1$^{-/-}$, or MyD88$^{-/-}$IFNAR1$^{-/-}$ mice were infected with *T. cruzi* for 6 h, washed to remove the extracellular parasites, and cultured for the indicated periods. The trypomastigotes in the culture supernatants were counted. Data are representative of four independent experiments. *B*, Peritoneal macrophages were infected with *T. cruzi*, washed, and cultured in the presence of [$^3$H]uracil for 72 h. The [$^3$H]uracil incorporation was then measured. *, $p < 0.0001$. *C* and *D*, Bone marrow-derived macrophages from each genotype were infected with *T. cruzi*, washed, and cultured for 48 h. The cells were then fixed, stained, and analyzed by microscopy. Representative stained cells from three independent experiments are shown. Magnification, ×400. Intracellular parasites were counted, and the data represent the mean + SD of the number of parasites per 250 macrophages. *, $p < 0.02$.

to those in MyD88$^{-/-}$TRIF$^{-/-}$ mice. We further monitored the mortality of the mice after *T. cruzi* infection (Fig. 6*B*). WT, TRIF$^{-/-}$, and IFNAR1$^{-/-}$ mice were resistant to *T. cruzi* infection, and all the mice survived for more than 19 days after the infection, whereas MyD88$^{-/-}$ mice started to die around 15 days after the infection, and about half of the mice had died within 19 days. In contrast, all the MyD88$^{-/-}$TRIF$^{-/-}$ and MyD88$^{-/-}$IFNAR1$^{-/-}$ mice died within 19 days of the infection. Thus, MyD88$^{-/-}$TRIF$^{-/-}$ and MyD88$^{-/-}$IFNAR1$^{-/-}$ mice were more sensitive to in vivo *T. cruzi* infection than MyD88$^{-/-}$ mice, suggesting that IFN-$\beta$ mediates in vivo resistance to *T. cruzi* infection, and this effect becomes evident in the absence of MyD88.

### *Involvement of IFN-β-inducible IRG47 in resistance to* T. cruzi *infection*

Next, we addressed the molecular mechanisms of the IFN-$\beta$-mediated resistance to *T. cruzi* infection in innate immune cells. The family of p47 GTPases has been shown to control innate immune responses to intracellular pathogens, including protozoan parasites (27, 28). In addition, expression of p47 GTPases, such as LRG47

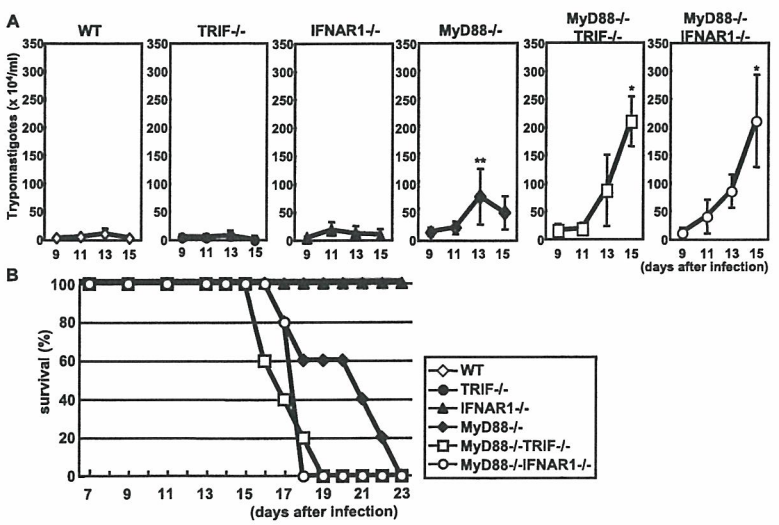


**FIGURE 6.** High-sensitivity MyD88$^{-/-}$IFNAR1$^{-/-}$ mice to *T. cruzi* infection. WT ($n$ = 9), TRIF$^{-/-}$ ($n$ = 10), IFNAR1$^{-/-}$ ($n$ = 10), MyD88$^{-/-}$ ($n$ = 5), MyD88$^{-/-}$TRIF$^{-/-}$ ($n$ = 5), and MyD88$^{-/-}$IFNAR1$^{-/-}$ ($n$ = 5) mice were i.p. infected with $1 \times 10^4$ *T. cruzi*. Parasitemia (*A*) and mortality (*B*) were monitored at the indicated times after infection. *, $p < 0.001$ compared with MyD88$^{-/-}$ mice and **, $p < 0.005$ compared with control mice.

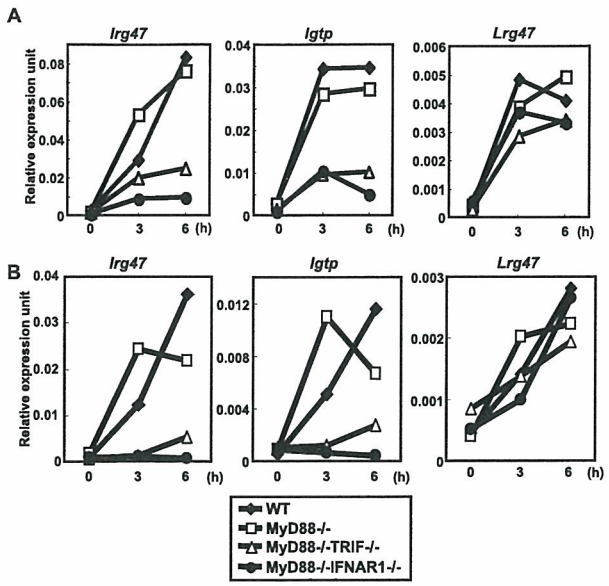


**FIGURE 7.** Impaired expression of IRG47 in *T. cruzi*-infected MyD88$^{-/-}$TRIF$^{-/-}$ mice. Bone marrow-derived macrophages (*A*) or DCs (*B*) from WT, MyD88$^{-/-}$, MyD88$^{-/-}$TRIF$^{-/-}$, or MyD88$^{-/-}$IFNAR1$^{-/-}$ mice were infected with *T. cruzi* for 3 or 6 h. Next, total RNA was extracted and analyzed for the expressions of *Irg47*, *Igtp*, *and Lrg47* by quantitative real-time RT-PCR. Data are shown as the relative mRNA levels normalized to the corresponding EF-1α mRNA level.

and IRG47, and inducibly expressed GTPase (IGTP), has been shown to be induced through activation of TLR and IFN signaling pathways during infection with intracellular pathogens (27, 28). Therefore, we analyzed the expression levels of these p47 GTPases in *T. cruzi*-infected DCs and macrophages. Bone marrow-derived macrophages or DCs from WT, MyD88$^{-/-}$, MyD88$^{-/-}$TRIF$^{-/-}$, and MyD88$^{-/-}$IFNAR1$^{-/-}$ mice were infected with *T. cruzi* for 3 or 6 h, and the expression of LRG47, IRG47, and IGTP mRNAs was analyzed (Fig. 7, *A* and *B*). In WT and MyD88$^{-/-}$ macrophages and DCs, *T. cruzi* infection resulted in robust mRNA expressions of all these p47 GTPases. Even in MyD88$^{-/-}$TRIF$^{-/-}$ and MyD88$^{-/-}$IFNAR1$^{-/-}$ cells, almost normal *T. cruzi*-induced expression of LRG47 mRNA was observed. However, *T. cruzi*-induced expression of IRG47 and IGTP mRNAs was severely impaired in MyD88$^{-/-}$TRIF$^{-/-}$ and MyD88$^{-/-}$IFNAR1$^{-/-}$ macrophages and DCs. Although IGTP was previously shown to have a minor role in *T. cruzi* infection, the involvement of IRG47 in *T. cruzi* infection is less well defined (29). Therefore, we next analyzed whether IRG47 is responsible for antitrypanosomal responses in the absence of MyD88. To complete this analysis, siRNA-mediated knockdown of IRG47 was performed in MyD88$^{-/-}$ macrophages. We transfected an IRG47 or control siRNA into bone marrow-derived macrophages and extracted the total RNA after 18 h for analysis of the IRG47 expression (Fig. 8*A*). Introduction of the IRG47 siRNA into bone marrow-derived macrophages from MyD88$^{-/-}$ mice resulted in an effective (81%) reduction in IRG47 mRNA expression. MyD88$^{-/-}$ macrophages transfected with the IRG47 or control siRNA were further infected with *T. cruzi*, and the intracellular parasites were visualized and counted (Fig. 8, *B* and *C*). In MyD88$^{-/-}$ macrophages, siRNA-mediated knockdown of IRG47 led to increased numbers of intracellular *T. cruzi*. These results indicate that IRG47 is involved in resistance to *T. cruzi* infection in innate immune cells.

## Discussion

In the present study, we analyzed innate immune responses to the intracellular protozoan parasite *T. cruzi* using MyD88$^{-/-}$TRIF$^{-/-}$ mice, in which TLR-dependent activation of innate immunity is not induced. Macrophages and DCs derived from MyD88$^{-/-}$TRIF$^{-/-}$ mice showed impaired clearance of *T. cruzi*. Analysis of the gene expression profiles of *T. cruzi*-infected MyD88$^{-/-}$TRIF$^{-/-}$ DCs revealed that IFN-β was induced in a TRIF-dependent manner during *T. cruzi* infection, whereas analyses with an anti-IFN-β neutralizing Ab and MyD88$^{-/-}$IFNAR1$^{-/-}$ cells demonstrated that IFN-β mediated antitrypanosomal innate immune responses. Furthermore, both MyD88$^{-/-}$TRIF$^{-/-}$ and MyD88$^{-/-}$IFNAR1$^{-/-}$ mice were highly sensitive to in vivo *T. cruzi* infection. These findings indicate that MyD88-dependent induction of proinflammatory cytokines and TRIF-dependent induction of IFN-β both contribute to innate immune responses to *T. cruzi* infection. We further showed that the p47 GTPase IRG47 is responsible for the resistance to *T. cruzi* infection in MyD88$^{-/-}$ macrophages.

Type I IFNs are well-known cytokines that exhibit antiviral activities (30). However, a large body of evidence has demonstrated

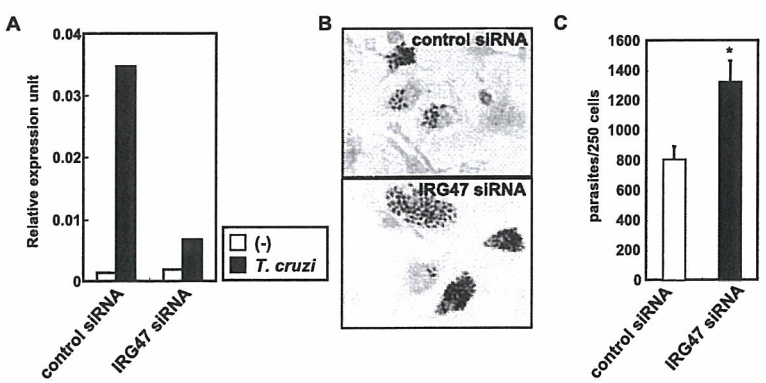


**FIGURE 8.** IRG47 mediates antitrypanosomal activity in MyD88$^{-/-}$ mice. *A*, Bone marrow-derived macrophages were transfected with IRG47 or control siRNA and cultured for 18 h. The cells were then infected with *T. cruzi* for 6 h and analyzed for the expression of IRG47 mRNA by quantitative real-time RT-PCR. Data are shown as the relative mRNA levels normalized to the corresponding EF-1α mRNA level. *B* and *C*, Bone marrow-derived macrophages transfected with an IRG47 or control siRNA were infected with *T. cruzi*, washed, and cultured for 48 h. The cells were then fixed, stained, and analyzed by microscopy. Representative stained cells from three independent experiments are shown. Magnification, ×400. Intracellular parasites were counted, and the data represent the mean + SD of the number of parasites per 250 macrophages. *, $p < 0.02$ compared with control siRNA-transfected cells.

that type I IFNs are also induced by nonviral pathogens, such as bacteria, mycobacteria, and protozoan parasites (11, 31). In the case of bacterial infection, type I IFNs seem to have opposing effects depending on the type of bacteria (31). Although exogenous type I IFNs show protective actions in response to infection with *Salmonella typhimurium* or *Shigella flexneri*, the protective effects of endogenous type I IFNs remain unclear (32, 33). In contrast, endogenous type I IFNs reduce resistance to *Listeria monocytogenes* infection (34–36). During infection with the protozoan parasite *Leishmania major*, these exogenous IFNs presumably have a protective effect through the induction of inducible NO synthase, although the involvement of endogenous type I IFNs in antileishmanial immunity is less clear (37, 38). Following infection with *T. cruzi*, administration of exogenous $\alpha\beta$ IFN was reported to reduce the number of serum parasites (10). However, a subsequent study showed that IFNAR1$^{-/-}$ mice were not susceptible to the infection, indicating that endogenous $\alpha\beta$ IFN do not contribute to the host defense against *T. cruzi* (39). Thus, the possible roles of type I IFNs in antitrypanosomal immune responses remain controversial. In the present study, we have clearly established that IFN-$\beta$ produced by DCs and macrophages contributes to host defense against *T. cruzi*. Thus, endogenous type I IFNs produced during *T. cruzi* infection are responsible for antitrypanosomal immune responses, although the MyD88-dependent production of proinflammatory cytokines overshadows the effects of type I IFNs in normal mice. In the future, it will be interesting to investigate whether this mechanism also applies to immune responses to other protozoan parasites, such as *L. major* and *Toxoplasma gondii*.

We further analyzed the mechanisms by which IFN-$\beta$ exerts antitrypanosomal responses. The p47 GTPase family members control innate immune responses to intracellular pathogens, including protozoan parasites (27, 28). Expression of p47 GTPases, such as LRG47 and IRG47, and of IGTP is induced through the activation of TLR and IFN signaling pathways during infection with intracellular pathogens. Mice lacking LRG47, IRG47, or IGTP have been shown to become sensitive to infection with *L. major* and *T. gondii*, indicating the possible involvement of these GTPases in *T. cruzi* infection (27, 40, 41). Indeed, LRG47-deficient mice have recently been shown to be sensitive to *T. cruzi* infection (42). We found that induction of IRG47 was impaired in *T. cruzi*-infected cells from MyD88$^{-/-}$TRIF$^{-/-}$ and MyD88$^{-/-}$IFNAR1$^{-/-}$ mice. Knockdown of IRG47 in MyD88$^{-/-}$ macrophages led to increased intracellular parasites. Thus, TLR-dependent expression of IFN-$\beta$ probably mediates antitrypanosomal responses through the induction of IRG47.

Recently, MyD88$^{-/-}$TRIF$^{-/-}$ macrophages have been shown to produce IFN-$\beta$ when infected with intracellular pathogens that escape into the cytosol, such as *L. monocytogenes* and *Legionella pneumophila* (43). In contrast, *T. cruzi*-induced IFN-$\beta$ production was not observed in MyD88$^{-/-}$TRIF$^{-/-}$ macrophages, although this parasite also invades the cytosol (44). In the case of the cytosolic escape of *Listeria* or *Legionella*, dsDNA from the bacteria is responsible for the induction of IFN-$\beta$ (43, 45). In contrast to these prokaryotic bacteria, *T. cruzi* is a eukaryote. Therefore, it seems less likely that trypanosomal DNA within the nucleus is exposed to the host cell cytosol, which may lead to the observed absence of TLR-independent induction of IFN-$\beta$. Thus, recognition of *T. cruzi* invasion is mainly dependent on TLR systems, possibly at the plasma membrane or in the phagolysosome. However, even in MyD88$^{-/-}$TRIF$^{-/-}$ macrophages, the gene encoding LRG47 was induced after *T. cruzi* infection, indicating the presence of TLR-independent mechanisms for gene expression. The mechanisms for the TLR-independent induction of this p47 GTPase are currently under investigation.

To date, TLR2, TLR4, and TLR9 have been implicated in the recognition of *T. cruzi*-derived components (6, 14–16). TLR2 recognizes GPI-anchored mucin-like proteins and the *T. cruzi*-released protein Tc52 (6, 46, 47), whereas TLR4 is responsible for the recognition of glycoinositolphospholipids (15). TLR9 is also involved in the recognition of the CpG motif present in *T. cruzi* DNA (14). Among these *T. cruzi*-derived components, glycoinositolphospholipids can activate the TRIF-dependent pathway to induce IFN-$\beta$ via TLR4. It is also possible that currently unknown components are recognized by TLR4 or TLR3, both of which use the TRIF-dependent pathway. Identification of such components responsible for the induction of IFN-$\beta$ would provide important insights toward understanding innate immune responses to *T. cruzi* infection.

## Acknowledgments

We thank Y. Yamada and K. Takeda for technical assistance, and M. Kurata for secretarial assistance.

## Disclosures

The authors have no financial conflict of interest.

## References

1. Krettli, A. U., and Z. Brener. 1982. Resistance against *Trypanosoma cruzi* associated to anti-living trypomastigote antibodies. *J. Immunol.* 128: 2009–2012.
2. Rottenberg, M., R. L. Cardoni, R. Andersson, E. L. Segura, and A. Orn. 1988. Role of T helper/inducer cells as well as natural killer cells in resistance to *Trypanosoma cruzi* infection. *Scand. J. Immunol.* 28: 573–582.
3. Tarleton, R. L. 1990. Depletion of CD8$^+$ T cells increases susceptibility and reverses vaccine-induced immunity in mice infected with *Trypanosoma cruzi*. *J. Immunol.* 144: 717–724.
4. Aliberti, J. C., M. A. Cardoso, G. A. Martins, R. T. Gazzinelli, L. Q. Vieira, and J. S. Silva. 1996. Interleukin-12 mediates resistance to *Trypanosoma cruzi* in mice and is produced by murine macrophages in response to live trypomastigotes. *Infect. Immun.* 64: 1961–1967.
5. Camargo, M. M., I. C. Almeida, M. E. Pereira, M. A. Ferguson, L. R. Travassos, and R. T. Gazzinelli. 1997. Glycosylphosphatidylinositol-anchored mucin-like glycoproteins isolated from *Trypanosoma cruzi* trypomastigotes initiate the synthesis of proinflammatory cytokines by macrophages. *J. Immunol.* 158: 5890–5901.
6. Ouaissi, A., E. Guilvard, Y. Delneste, G. Caron, G. Magistrelli, N. Herbault, N. Thieblemont, and P. Jeannin. 2002. The *Trypanosoma cruzi* Tc52-released protein induces human dendritic cell maturation, signals via Toll-like receptor 2, and confers protection against lethal infection. *J. Immunol.* 168: 6366–6374.
7. Reed, S. G. 1988. In vivo administration of recombinant IFN-$\gamma$ induces macrophage activation, and prevents acute disease, immune suppression, and death in experimental *Trypanosoma cruzi* infections. *J. Immunol.* 140: 4342–4347.
8. Silva, J. S., P. J. Morrissey, K. H. Grabstein, K. M. Mohler, D. Anderson, and S. G. Reed. 1992. Interleukin 10 and interferon $\gamma$ regulation of experimental *Trypanosoma cruzi* infection. *J. Exp. Med.* 175: 169–174.
9. Sonnenfeld, G., and F. Kierszenbaum. 1981. Increased serum levels of an interferon-like activity during the acute period of experimental infection with different strains of *Trypanosoma cruzi*. *Am. J. Trop. Med. Hyg.* 30: 1189–1191.
10. Kierszenbaum, F., and G. Sonnenfeld. 1982. Characterization of the antiviral activity produced during *Trypanosoma cruzi* infection and protective effects of exogenous interferon against experimental Chagas' disease. *J. Parasitol.* 68: 194–198.
11. Bogdan, C., J. Mattner, and U. Schleicher. 2004. The role of type I interferons in non-viral infections. *Immunol. Rev.* 202: 33–48.
12. Takeda, K., T. Kaisho, and S. Akira. 2003. Toll-like receptors. *Annu. Rev. Immunol.* 21: 335–376.
13. Akira, S., and K. Takeda. 2004. Toll-like receptor signalling. *Nat. Rev. Immunol.* 4: 499–511.
14. Shoda, L. K., K. A. Kegerreis, C. E. Suarez, I. Roditi, R. S. Corral, G. M. Bertot, J. Norimine, and W. C. Brown. 2001. DNA from protozoan parasites *Babesia bovis*, *Trypanosoma cruzi*, and *T. brucei* is mitogenic for B lymphocytes and stimulates macrophage expression of interleukin-12, tumor necrosis factor $\alpha$, and nitric oxide. *Infect. Immun.* 69: 2162–2171.
15. Oliveira, A.-C., J. R. Peixoto, L. B. de Arruda, M. A. Campos, R. T. Gazzinelli, D. T. Golenbock, S. Akira, J. O. Previato, L. Mendonça-Previato, A. Nobrega, and M. Bellio. 2004. Expression of functional TLR4 confers proinflammatory responsiveness to *Trypanosoma cruzi* glycoinositolphospholipids and higher resistance to infection with *T. cruzi*. *J. Immunol.* 173: 5688–5696.
16. Petersen, C. A., K. A. Krumholz, and B. A. Burleigh. 2005. Toll-like receptor 2 regulates interleukin-1$\beta$-dependent cardiomyocyte hypertrophy triggered by *Trypanosoma cruzi*. *Infect. Immun.* 73: 6974–6980.
17. Campos, M. A., M. Closel, E. P. Valente, J. E. Cardoso, S. Akira, J. I. Alvarez-Leite, C. Ropert, and R. T. Gazzinelli. 2004. Impaired production of proinflammatory cytokines and host resistance to acute infection with *Trypanosoma cruzi* in mice lacking functional myeloid differentiation factor 88. *J. Immunol.* 172: 1711–1718.

18. Adachi, O., T. Kawai, K. Takeda, M. Matsumoto, H. Tsutsui, M. Sakagami, K. Nakanishi, and S. Akira. 1998. Targeted disruption of the MyD88 gene results in loss of IL-1- and IL-18-mediated function. *Immunity* 9: 143–150.
19. Yamamoto, M., S. Sato, H. Hemmi, K. Hoshino, T. Kaisho, H. Sanjo, O. Takeuchi, M. Sugiyama, M. Okabe, K. Takeda, and S. Akira. 2003. Role of adaptor TRIF in the MyD88-independent Toll-like receptor signaling pathway. *Science* 301: 640–643.
20. Müller, U., U. Steinhoff, L. F. Reis, S. Hemmi, J. Pavlovic, R. M. Zinkernagel, and M. Aguet. 1994. Functional role of type I and type II interferons in antiviral defense. *Science* 264: 1918–1921.
21. Taliaferro, W. H., and T. Pizzi. 1955. Connective tissue reactions in normal and immunized mice to a reticulotropic strain of *Trypanosoma cruzi*. *J. Infect. Dis.* 96: 199–226.
22. Vespa, G. N., F. Q. Cunha, and J. S. Silva. 1994. Nitric oxide is involved in control of *Trypanosoma cruzi*-induced parasitemia and directly kills the parasite in vitro. *Infect. Immun.* 62: 5177–5182.
23. Saeftel, M., B. Fleischer, and A. Hoerauf. 2001. Stage-dependent role of nitric oxide in control of *Trypanosoma cruzi* infection. *Infect. Immun.* 69: 2252–2259.
24. Silva, J. S., G. N. Vespa, M. A. Cardoso, J. C. Aliberti, and F. Q. Cunha. 1995. Tumor necrosis factor α mediates resistance to *Trypanosoma cruzi* infection in mice by inducing nitric oxide production in infected γ interferon-activated macrophages. *Infect. Immun.* 63: 4862–4867.
25. Castaños-Velez, E., S. Maerlan, L. M. Osorio, F. Åberg, P. Biberfeld, A. Örn, and M. E. Rottenberg. 1998. *Trypanosoma cruzi* infection in tumor necrosis factor receptor p55-deficient mice. *Infect. Immun.* 66: 2960–2968.
26. Ortiz-Ortiz, L., T. Ortega, R. Capin, and T. Martinez. 1976. Enhanced mononuclear phagocytic activity during *Trypanosoma cruzi* infection in mice. *Int. Arch. Allergy Appl. Immunol.* 50: 232–242.
27. Taylor, G. A., C. G. Feng, and A. Sher. 2004. p47 GTPases: regulators of immunity to intracellular pathogens. *Nat. Rev. Immunol.* 4: 100–109.
28. MacMicking, J. D. 2005. Immune control of phagosomal bacteria by p47 GTPases. *Curr. Opin. Microbiol.* 8: 74–82.
29. de Souza, A. P., B. Tang, H. B. Tanowitz, S. M. Factor, V. Shtutin, J. Shirani, G. A. Taylor, L. M. Weiss, and L. A. Jelicks. 2003. Absence of interferon-γ-inducible gene IGTP does not significantly alter the development of chagasic cardiomyopathy in mice infected with *Trypanosoma cruzi* (Brazil strain). *J. Parasitol.* 89: 1237–1239.
30. Isaacs, A., and J. Lindenmann. 1957. Virus interference. I. The interferon. *Proc. R. Soc. Lond. B. Biol. Sci.* 147: 258–267.
31. Decker, T., M. Müller, and S. Stockinger. 2005. The Yin and Yang of type I interferon activity in bacterial infection. *Nat. Rev. Immunol.* 5: 675–687.
32. Hess, C. B., D. W. Niesel, Y. J. Cho, and G. R. Klimpel. 1987. Bacterial invasion of fibroblasts induces interferon production. *J. Immunol.* 138: 3949–3953.
33. Niesel, D. W., C. B. Hess, Y. J. Cho, K. D. Klimpel, and G. R. Klimpel. 1986. Natural and recombinant interferons inhibit epithelial cell invasion by Shigella spp. *Infect. Immun.* 52: 828–833.
34. O'Connell, R. M., S. K. Saha, S. A. Vaidya, K. W. Bruhn, G. A. Miranda, B. Zarnegar, A. K. Perry, B. O. Nguyen, T. F. Lane, T. Taniguchi, et al. 2004. Type I interferon production enhances susceptibility to *Listeria monocytogenes* infection. *J. Exp. Med.* 200: 437–445.
35. Carrero, J. A., B. Calderon, and E. R. Unanue. 2004. Type I interferon sensitizes lymphocytes to apoptosis and reduces resistance to *Listeria* infection. *J. Exp. Med.* 200: 535–540.
36. Auerbuch, V., D. G. Brockstedt, N. Meyer-Morse, M. O'Riordan, and D. A. Portnoy. 2004. Mice lacking the type I interferon receptor are resistant to *Listeria monocytogenes*. *J. Exp. Med.* 200: 527–533.
37. Diefenbach, A., H. Schindler, N. Donhauser, E. Lorenz, T. Laskay, J. MacMicking, M. Rollinghoff, I. Gresser, and C. Bogdan. 1998. Type 1 interferon (IFNα/β) and type 2 nitric oxide synthase regulate the innate immune response to a protozoan parasite. *Immunity* 8: 77–87.
38. Mattner, J., A. Wandersee-Steinhauser, A. Pahl, M. Rollinghoff, G. R. Majeau, P. S. Hochman, and C. Bogdan. 2004. Protection against progressive leishmaniasis by IFN-β. *J. Immunol.* 172: 7574–7582.
39. Une, C., J. Andersson, and A. Orn. 2003. Role of IFN-α/β and IL-12 in the activation of natural killer cells and interferon-γ production during experimental infection with *Trypanosoma cruzi*. *Clin. Exp. Immunol.* 134: 195–201.
40. Taylor, G. A., C. M. Collazo, G. S. Yap, K. Nguyen, T. A. Gregorio, L. S. Taylor, B. Eagleson, L. Secrest, E. A. Southon, S. W. Reid, et al. 2000. Pathogen-specific loss of host resistance in mice lacking the IFN-γ-inducible gene IGTP. *Proc. Natl. Acad. Sci. USA* 97: 751–755.
41. Collazo, C. M., G. S. Yap, G. D. Sempowski, K. C. Lusby, L. Tessarollo, G. F. Woude, A. Sher, and G. A. Taylor. 2001. Inactivation of LRG-47 and IRG-47 reveals a family of interferon γ-inducible genes with essential, pathogen-specific roles in resistance to infection. *J. Exp. Med.* 194: 181–188.
42. Santiago, H. C., C. G. Feng, A. Bafica, E. Roffe, R. M. Arantes, A. Cheever, G. Taylor, L. Q. Vierira, J. Aliberti, R. T. Gazzinelli, and A. Sher. 2005. Mice deficient in LRG-47 display enhanced susceptibility to *Trypanosoma cruzi* infection associated with defective hemopoiesis and intracellular control of parasite growth. *J. Immunol.* 175: 8165–8172.
43. Stetson, D. B., and R. Medzhitov. 2006. Recognition of cytosolic DNA activates an IRF3-dependent innate immune response. *Immunity* 24: 93–103.
44. Andrade, L. O., and N. W. Andrews. 2004. Lysosomal fusion is essential for the retention of *Trypanosoma cruzi* inside host cells. *J. Exp. Med.* 200: 1135–1143.
45. Ishii, K. J., C. Coban, H. Kato, K. Takahashi, Y. Torii, F. Takeshita, H. Ludwig, G. Sutter, K. Suzuki, H. Hemmi, et al. 2006. A Toll-like receptor-independent antiviral response induced by double-stranded B-form DNA. *Nat. Immunol.* 7: 40–48.
46. Campos, M. A., I. C. Almeida, O. Takeuchi, S. Akira, E. P. Valente, D. O. Procopio, L. R. Travassos, J. A. Smith, D. T. Golenbock, and R. T. Gazzinelli. 2001. Activation of Toll-like receptor-2 by glycosylphosphatidylinositol anchors from a protozoan parasite. *J. Immunol.* 167: 416–423.
47. Ropert, C., I. C. Almeida, M. Closel, L. R. Travassos, M. A. Ferguson, P. Cohen, and R. T. Gazzinelli. 2001. Requirement of mitogen-activated protein kinases and IκB phosphorylation for induction of proinflammatory cytokines synthesis by macrophages indicates functional similarity of receptors triggered by glycosylphosphatidylinositol anchors from parasitic protozoa and bacterial lipopolysaccharide. *J. Immunol.* 166: 3423–3431.

nature immunology



# Detection of pathogenic intestinal bacteria by Toll-like receptor 5 on intestinal CD11c$^+$ lamina propria cells

Satoshi Uematsu[1,7], Myoung Ho Jang[2,7], Nicolas Chevrier[1], Zijin Guo[2], Yutaro Kumagai[1], Masahiro Yamamoto[1], Hiroki Kato[1], Nagako Sougawa[2], Hidenori Matsui[3], Hirotaka Kuwata[4], Hiroaki Hemmi[1], Cevayir Coban[5], Taro Kawai[6], Ken J Ishii[6], Osamu Takeuchi[1,6], Masayuki Miyasaka[2], Kiyoshi Takeda[4] & Shizuo Akira[1,6]

**Toll-like receptors (TLRs) recognize distinct microbial components and induce innate immune responses. TLR5 is triggered by bacterial flagellin. Here we generated *Tlr5*$^{-/-}$ mice and assessed TLR5 function *in vivo*. Unlike other TLRs, TLR5 was not expressed on conventional dendritic cells or macrophages. In contrast, TLR5 was expressed mainly on intestinal CD11c$^+$ lamina propria cells (LPCs). CD11c$^+$ LPCs detected pathogenic bacteria and secreted proinflammatory cytokines in a TLR5-dependent way. However, CD11c$^+$ LPCs do not express TLR4 and did not secrete proinflammatory cytokines after exposure to a commensal bacterium. Notably, transport of pathogenic *Salmonella typhimurium* from the intestinal tract to mesenteric lymph nodes was impaired in *Tlr5*$^{-/-}$ mice. These data suggest that CD11c$^+$ LPCs, via TLR5, detect and are used by pathogenic bacteria in the intestinal lumen.**

Toll-like receptors (TLRs) recognize a variety of pathogen-associated molecular patterns and induce innate immune responses[1]. TLRs are abundantly expressed on 'professional' antigen-presenting cells such as macrophages and dendritic cells (DCs) and serve as an important link between the innate and adaptive immune responses. So far, 13 TLRs have been identified in mammals. Among the TLR family members, TLR5 was the first to be shown to recognize a protein ligand, bacterial flagellin[2]. Bacterial flagellin is a structural protein that forms the main portion of flagella, which promote bacterial chemotaxis and bacterial adhesion to and invasion of host tissues[3]. Flagellin of *Listeria monocytogenes* and *Salmonella typhimurium* stimulates TLR5 (ref. 4). Thus, TLR5 recognizes flagellin from both Gram-positive and Gram-negative bacteria. *In vitro* studies have shown that TLR5 recognizes the conserved domain in flagellin monomers and triggers proinflammatory as well as adaptive immune responses[5]. In addition, TLR5 is expressed on the basolateral surface of intestinal epithelial cells and is thought to be key in the recognition of invasive flagellated bacteria at the mucosal surface[4]. When exposed to flagellin, human intestinal epithelial cell lines produce chemokines that induce subsequent migration of immature DCs[6]. There is high expression of TLR5 in the human lung[7], and a correlation between a common human TLR5 polymorphism and susceptibility to legionellosis has been identified[8]. Although accumulating evidence suggests that TLR5 is an important sensor for flagellated pathogens, the *in vivo* function of TLR5 is yet to be elucidated.

Here we generated *Tlr5*$^{-/-}$ mice and examined the function of TLR5 *in vivo* in the intestine. We confirmed that flagellin is a natural ligand for TLR5. Although it is known that *in vivo* administration of flagellin induces inflammatory cytokine production, it remains unclear which cell populations produce those cytokines. Because it is known that there is high expression of TLR5 in the intestine, we first isolated and examined intestinal epithelial cells (IECs). Unexpectedly, TLR5 expression in IECs was much lower than that in the whole intestine. Consistent with that, IECs did not produce inflammatory cytokines in response to flagellin. Using a new method for isolating intestinal lamina propria cells (LPCs)[9], we found that CD11c$^+$ LPCs 'preferentially' expressed TLR5 and produced inflammatory cytokines after exposure to flagellin. CD11c$^+$ LPCs sensed pathogenic flagellated bacteria via TLR5 and induced inflammatory responses. In contrast, CD11c$^+$ LPCs do not express TLR4 and did not produce proinflammatory cytokines in response to a commensal bacterium. Although TLR5 initially induced host defenses against flagellated bacteria, *Tlr5*$^{-/-}$ mice were resistant to oral *S. typhimurium* infection. The transport of *S. typhimurium* from the intestinal tract to the mesenteric

[1]Department of Host Defense, Research Institute for Microbial Diseases, Osaka University, Suita Osaka 565-0871, Japan. [2]Laboratory of Immunodynamics, Department of Microbiology and Immunology, Osaka University Graduate School of Medicine (C8), 2-2, Yamada-oka, Suita, 565-0871, Japan. [3]Laboratory of Immunoregulation, Kitasato Institute for Life Sciences and Graduate School of Infection, Control Sciences, Kitasato University, 5-9-1 Shirokane, Minato-ku, Tokyo 108-8641, Japan. [4]Department of Molecular Genetics, Medical Institute of Bioregulation, Kyushu University, 3-1-1 Maidashi, Higashi-ku, Fukuoka 812-8582, Japan. [5]21st Century COE, Combined Program on Microbiology and Immunology, Osaka University, 3-1 Yamada-oka, Suita Osaka 565-0871, Japan. [6]ERATO, Japan Science and Technology Corporation, 3-1 Yamada-oka, Suita Osaka 565-0871, Japan. [7]These authors contributed equally to this work. Correspondence should be addressed to S.A. (sakira@biken.osaka-u.ac.jp).

Received 28 March; accepted 13 June; published online 9 July 2006; doi:10.1038/ni1362

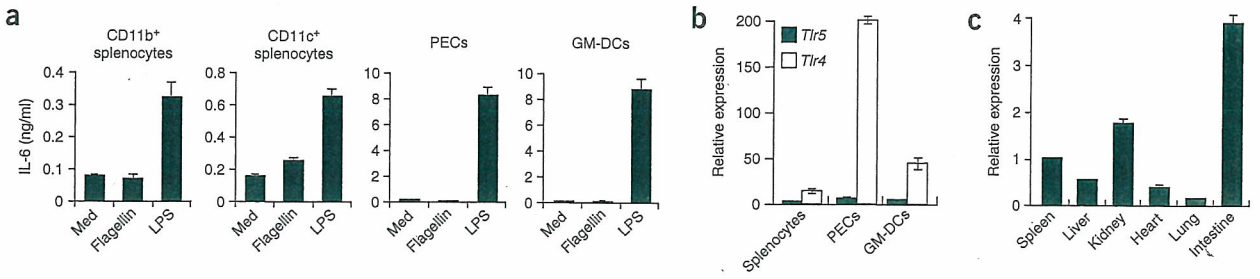


**Figure 1** Macrophages and conventional DCs are hyporesponsive to flagellin. (**a**) Enzyme-linked immunosorbent assay of IL-6 production by splenic CD11b$^+$ and CD11c$^+$ cells, GM-DCs and peritoneal macrophages (PECs) from C57BL/6 mice. Cells were cultured with medium only (Med), flagellin (1 μg/ml) or LPS (100 ng/ml). (**b**,**c**) Quantitative real-time PCR of *Tlr5* and *Tlr4* expression in various cell types (**b**) or organs (**c**) of C57BL/6 mice. Data are mean ± s.d. of triplicate samples from one representative of three independent experiments.

lymph nodes (MLNs) was impaired in *Tlr5*$^{-/-}$ mice. These results suggest that TLR5$^+$CD11c$^+$ LPCs detect and can be used by pathogenic bacteria in the intestine.

## RESULTS

### Flagellin is a natural ligand for TLR5

To elucidate the physiological function of TLR5, we generated *Tlr5*$^{-/-}$ mice by gene targeting. Mouse *Tlr5* consists of one exon. We constructed the targeting vector to allow insertion of a neomycin-resistance gene cassette into that exon (**Supplementary Fig. 1**). We microinjected two correctly targeted embryonic stem clones into C57BL/6 blastcysts to generate chimeric mice. We crossed chimeric male mice with C57BL/6 female mice and monitored transmission of the mutated allele by Southern blot analysis (**Supplementary Fig. 1**). We then interbred heterozygous mice to produce offspring carrying the null mutation of *Tlr5*. *Tlr5*$^{-/-}$ mice were born at the expected mendelian ratio and showed no developmental abnormalities. To confirm the disruption of *Tlr5*, we analyzed total intestinal RNA from *Tlr5*$^{+/+}$ and *Tlr5*$^{-/-}$ mice by RNA blot and detected no *Tlr5* transcripts in *Tlr5*$^{-/-}$ intestinal RNA (**Supplementary Fig. 1**).

To assess the involvement of TLR5 in the systemic production of proinflammatory cytokines in response to flagellin, we measured the concentrations of interleukin 6 (IL-6) and IL-12p40 in sera of *Tlr5*$^{+/+}$ and *Tlr5*$^{-/-}$ mice at various time points after intraperitoneal injection of purified flagellin. Although IL-6 and IL-12p40 concentrations in the serum increased within 2 h of injection in *Tlr5*$^{+/+}$ mice, their concentrations remained low even at 4 h after injection in *Tlr5*$^{-/-}$ mice (**Supplementary Fig. 1**). These results confirmed that flagellin is a natural ligand for TLR5.

### Immune cell responses to flagellin

We next analyzed flagellin-mediated immune responses in macrophages and conventional DCs. We isolated CD11b$^+$ or CD11c$^+$ splenocytes, peritoneal macrophages and granulocyte-macrophage colony stimulating factor–induced bone marrow–derived DCs (GM-DCs) from *Tlr5*$^{+/+}$ mice, stimulated these cells with flagellin or the TLR4 ligand lipopolysaccharide (LPS) and measured IL-6 concentrations in cell culture supernatants (**Fig. 1a**). All cell types produced IL-6 after stimulation with LPS, but IL-6 production was not induced by stimulation with flagellin. In agreement with those results, splenocytes, peritoneal macrophages and GM-DCs had high expression of *Tlr4* but not *Tlr5* mRNA, as determined by quantitative real-time PCR (**Fig. 1b**). To identify the tissues involved in flagellin-induced production of proinflammatory cytokines, we measured *Tlr5* mRNA in the spleen, liver, kidney, heart, lung and intestine by quantitative real-time PCR and found that intestine had the highest expression of *Tlr5* mRNA (**Fig. 1c**).

TLR5 expression is confined to the basolateral surface of IECs[4]. To examine TLR5-mediated inflammatory responses in IECs, we isolated IECs from *Tlr5*$^{+/+}$ and *Tlr5*$^{-/-}$ mice, stimulated them with flagellin and used cDNA microarray to examine the profile of genes induced by TLR5 stimulation (**Fig. 2**). It has been reported that flagellin induces expression of genes encoding some chemokines (such as IL-8 and CCL20) in human IEC lines[6,10]. Our analyses showed flagellin-induced expression of some genes encoding proteins involved in immune responses, such as defensin-β3, CD86, killer cell lectin-like receptor subfamily A member 6, complement component 8α and

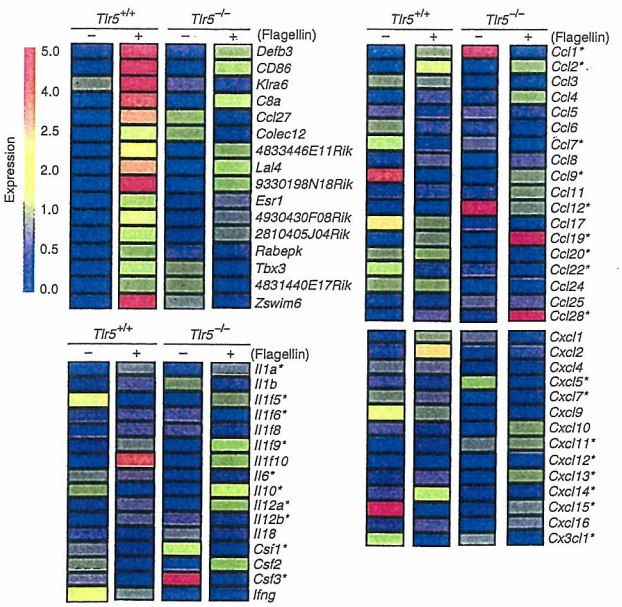


**Figure 2** Gene expression induced by flagellin stimulation in IECs. Microarray analysis of IECs from *Tlr5*$^{+/+}$ and *Tlr5*$^{-/-}$ mice stimulated with medium alone (–) or 1 μg/ml of flagellin (+). *, genes judged as being statistically undetectable at all time points. There is flagellin-induced expression of the genes encoding defensin-β3 (*Defb3*), CD86 (*Cd86*), killer cell lectin-like receptor subfamily A member 6 (*Klra6*), complement component 8α (*C8a*) and chemokine (C-C motif) ligand 27 (*Ccl27*) in *Tlr5*$^{+/+}$ but not *Tlr5*$^{-/-}$ IECs. Data are representative of three independent experiments.

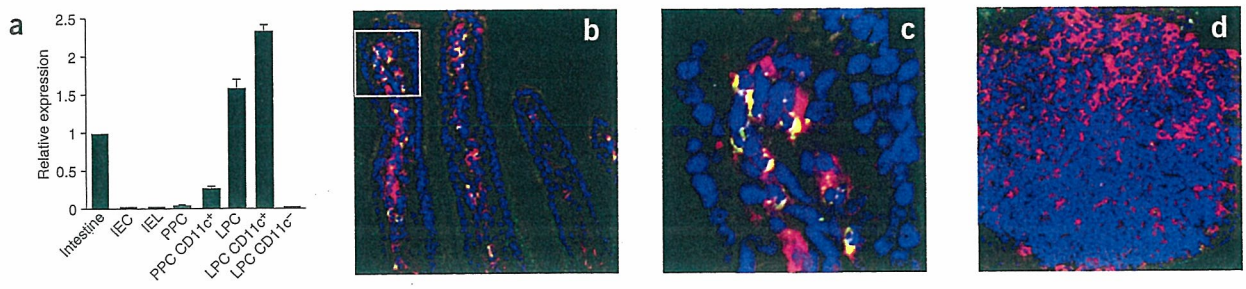


**Figure 3** TLR5 is highly expressed on CD11c$^+$ LPCs. (**a**) Quantitative real-time PCR of *Tlr5* expression by the intestine (far left) and by various cell types of C57BL/6 mice. IEL, intestinal epithelial lymphocyte. Data are mean ± s.d. of triplicate samples from one representative of three independent experiments. (**b–d**) Confocal microscopy of frozen tissue sections of small intestine (**b,c**) and Peyer's patch (**d**) of C57BL/6 mice, fixed and stained with antibodies specific for CD11c (red) and TLR5 (green). Image in **c** is an enlargement of the boxed area in **b**. Original magnification ×400 (**b,d**) and ×1,000 (**c**). Data are from one of three representative experiments.

chemokine (C-C motif) ligand 27 in *Tlr5*$^{+/+}$ but not *Tlr5*$^{-/-}$ IECs. However, most genes encoding chemokines were not induced by flagellin, even in *Tlr5*$^{+/+}$ IECs, and flagellin did not induce the expression of any genes encoding proinflammatory cytokines in *Tlr5*$^{+/+}$ IECs. We confirmed that *Tlr5*$^{+/+}$ IECs did not produce proinflammatory cytokine protein after flagellin stimulation (data not shown). There was much less *Tlr5* mRNA in IECs than in the entire small intestine (**Fig. 3a**).

Because TLR5 expression was low in IECs but high in the entire small intestine, we hypothesized that TLR5 must be 'preferentially' expressed in other intestinal cell types. We measured *Tlr5* mRNA in Peyer's patch cells (PPCs), intestinal epithelial lymphocytes and LPCs (**Fig. 3a**). There was high expression of *Tlr5* mRNA in LPCs, but *Tlr5* mRNA expression in intestinal epithelial lymphocytes and PPCs was lower than that in the entire small intestine. DCs are a dominant antigen-presenting cell in the lamina propria of mouse small bowel[11]. Therefore, we separated CD11c$^+$ cells from LPCs and PPCs and measured expression of *Tlr5* mRNA. We detected considerable *Tlr5* mRNA in CD11c$^+$ LPCs but not CD11c$^-$ LPCs. CD11c$^+$ PPCs had less *Tlr5* mRNA than did CD11c$^+$ LPCs. Next we examined the localization of TLR5 protein in the small intestine by immunohistochemistry. In agreement with the mRNA expression data, there was high expression of TLR5 on intestinal CD11c$^+$ LPCs (**Fig. 3b,c**) but not on PPCs (**Fig. 3d**). Thus, TLR5 is expressed specifically on CD11c$^+$ LPCs in the small intestine.

Next we assessed the effect of flagellin stimulation on CD11c$^+$ LPCs. *Tlr5*$^{+/+}$ but not *Tlr5*$^{-/-}$ CD11c$^+$ LPCs produced IL-6 and IL-12p40 in response to flagellin (**Fig. 4**, top). However, CD11c$^+$ LPCs did not produce large amounts of tumor necrosis factor after stimulation with flagellin and failed to produce any cytokines after LPS stimulation.

Antigen-presenting cells in Peyer's patches have been extensively characterized[12]. Peyer's patches contain unusual subsets of DCs that are important in the generation of regulatory T cells and the induction of oral tolerance[12,13]. These Peyer's patch DCs produce IL-10 in response to inflammatory stimulations such as LPS[14]. Consistent with their low expression of *Tlr5* mRNA (**Fig. 3a**), CD11c$^+$ PPCs did not produce inflammatory cytokines after stimulation with flagellin (**Fig. 4**, bottom). However, CD11c$^+$ PPCs produced IL-6 and IL-10 in response to LPS. In contrast, neither *Tlr5*$^{+/+}$ nor *Tlr5*$^{-/-}$ CD11c$^+$ LPCs produced IL-10 in response to flagellin, suggesting that in CD11c$^+$ LPCs, TLR5 signaling induces inflammatory responses but not tolerance (**Fig. 4**).

To comprehensively examine TLR5-mediated innate immune responses in the small intestine, we obtained RNA from *Tlr5*$^{+/+}$ and *Tlr5*$^{-/-}$ LPCs stimulated for 4 h with flagellin and hybridized the RNA to cDNA microarrays (**Fig. 5**). Several transcripts were substantially upregulated at 4 h after flagellin stimulation in *Tlr5*$^{+/+}$ but not *Tlr5*$^{-/-}$ LPCs. These included genes encoding proinflammatory molecules such as cytokines, cytokine receptors, chemokines, signaling molecules, prostanoids, prostanoid synthetase and secretary antimicrobial peptides (**Fig. 5**, top). Genes associated with cellular adhesion,

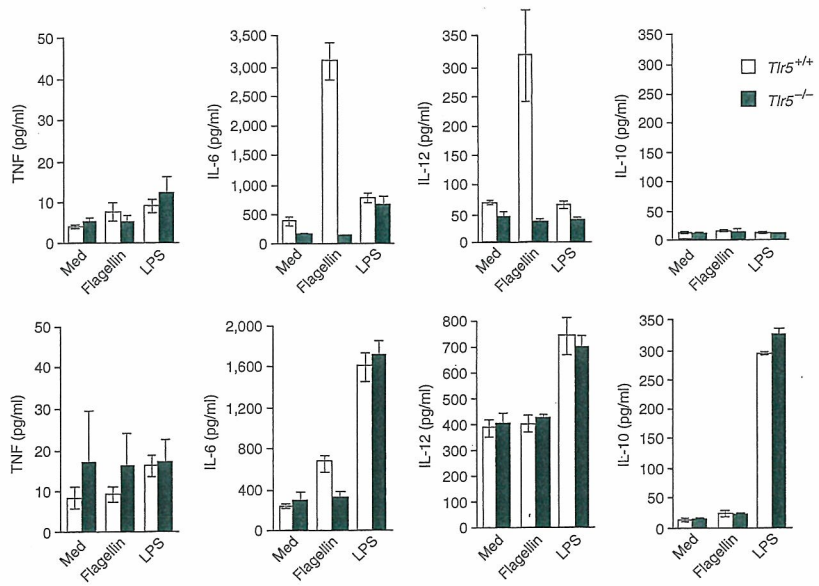


**Figure 4** TLR5-mediated CD11c$^+$ LPC cytokine production. Enzyme-linked immunosorbent assay of cytokine production by CD11c$^+$ LPCs (top) and PPCs (bottom) from *Tlr5*$^{+/+}$ and *Tlr5*$^{-/-}$ mice. Cells were cultured with medium only, flagellin (1 μg/ml) or LPS (100 ng/ml). Data are mean ± s.d. of triplicate samples from one representative of three independent experiments.

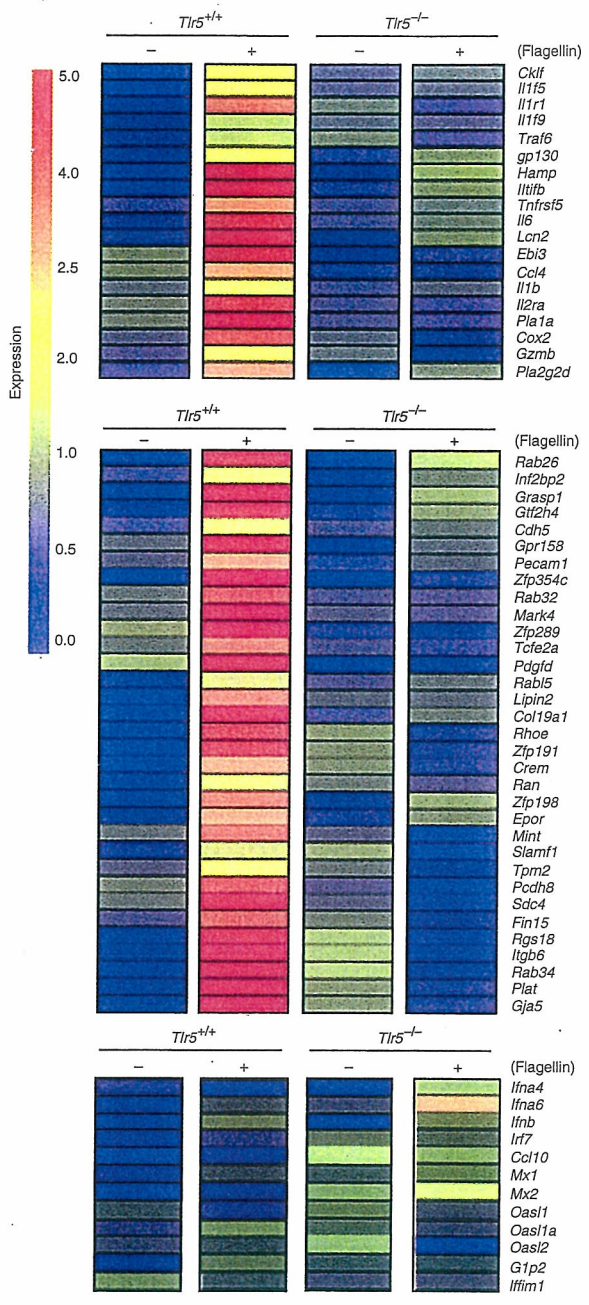


**Figure 5** Flagellin-induced gene expression in CD11c$^+$ LPCs. Microarray analysis of CD11c$^+$ LPCs from *Tlr5*$^{+/+}$ and *Tlr5*$^{-/-}$ mice left unstimulated (–) or stimulated with 1 μg/ml of flagellin (+). Upregulated genes encode cytokines (*Il6, Il1f5, Il1f9, Il1b, Ebi3* and *Iltifb*), cytokine receptors (*Tnfrsf5, Il1r1* and *Il2ra*), chemokines (*Cklf* and *Ccl4*), signaling molecules (*Traf6* and *gp130*), prostanoids (*Pla1a* and *Pla2g2d*), prostanoid synthetase (*Cox2*) and secretary antimicrobial peptides (*Hamp, Lcn* and *Gzmb*; top), as well as molecules associated with cellular adhesion, cytoskeletal organization, intracellular transport, vesicle fusion and transcription (middle). Data are representative of three independent experiments.

cytoskeletal organization, intracellular transport, vesicle fusion and transcription were also upregulated by flagellin stimulation (**Fig. 5**, middle). In contrast, interferon and interferon-inducible genes were not induced in response to flagellin in either *Tlr5*$^{+/+}$ or *Tlr5*$^{-/-}$ LPCs (**Fig. 5**, bottom).

### CD11c$^+$ LPCs detect pathogenic bacteria via TLR5

CD11c$^+$ LPCs produced IL-6 and IL-12p40 in response to flagellin but not LPS stimulation. CD11c$^+$ LPCs produced similar amounts of IL-6 when stimulated through TLR2 or TLR9 (**Supplementary Fig. 2** online), suggesting that LPS signaling is suppressed specifically in CD11c$^+$ LPCs. Therefore, we measured TLR4 and TLR5 in CD11c$^+$ LPCs and CD11c$^+$ splenic cells (SPCs; **Fig. 6a**). *Tlr4* expression was high and *Tlr5* expression was low in CD11c$^+$ SPCs. In contrast, *Tlr4* expression was low and *Tlr5* expression was high in CD11c$^+$ LPCs.

As CD11c$^+$ LPCs and SPCs had different expression profiles for TLR4 and TLR5, we assessed their responses to commensal and pathogenic bacteria. We isolated CD11c$^+$ LPCs and CD11c$^+$ SPCs from wild-type, *Tlr4*$^{-/-}$ and *Tlr5*$^{-/-}$ mice and measured IL-6 production induced by stimulation with heat-killed commensal Gram-negative bacteria (*Enterobacter cloacae*) and pathogenic Gram-negative bacteria (*S. typhimurium*; **Fig. 6b**). Wild type and *Tlr5*$^{-/-}$ CD11c$^+$ SPCs produced copious IL-6 in response to both *E. cloacae* and *S. typhimurium*. However, *Tlr4*$^{-/-}$ CD11c$^+$ SPCs produced less IL-6 than did wild-type or *Tlr5*$^{-/-}$ CD11c$^+$ SPCs, suggesting that CD11c$^+$ SPCs induce innate immune responses to Gram-negative bacteria mainly via TLR4. Wild-type and *Tlr4*$^{-/-}$ CD11c$^+$ LPCs produced copious IL-6 in response to *S. typhimurium*. In contrast, *Tlr5*$^{-/-}$ CD11c$^+$ LPCs produced little IL-6 after stimulation with *S. typhimurium*. We further assessed the response of CD11c$^+$ LPCs with a mutant strain of *S. typhimurium* that lacks the *fliA* gene and therefore does not produce flagella[15]. Wild-type and *Tlr5*$^{-/-}$ CD11c$^+$ LPCs were hyporesponsive to this *fliA* mutant (compared with their response to wild-type *S. typhimurium*), suggesting that CD11c$^+$ LPCs induce immune responses after recognizing flagellin of *S. typhimurium*. Unlike wild-type CD11c$^+$ SPCs, wild-type CD11c$^+$ LPCs produced a relatively small amount of IL-6 after stimulation with *E. cloacae*. These data suggest that CD11c$^+$ LPCs detect pathogenic flagellated bacteria and induce innate immune responses via TLR5.

### *S. typhimurium* uses TLR5 for systemic infection

To investigate whether TLR5 has a specific function in fighting bacterial infection in the intestine, we orally infected *Tlr5*$^{+/+}$ and *Tlr5*$^{-/-}$ mice with *S. typhimurium*. Unexpectedly, when assessed on a mixed genetic background (C56BL/6 × 129Sv, F2), all *Tlr5*$^{-/-}$ mice survived a dose of *S. typhymurium* that was lethal for *Tlr5*$^{+/+}$ mice (**Fig. 7a**, left). Next we assessed the resistance of *Tlr5*$^{-/-}$ mice backcrossed onto the C57BL/6 genetic background. Although wild-type C57BL/6 mice are resistant to oral *S. typhymurium* infection, *Tlr5*$^{-/-}$ C57BL/6 mice background were significantly more resistant, even at an extremely high dose ($5 \times 10^8$ bacteria; **Fig. 7a**, right). These results indicate that *Tlr5*$^{-/-}$ mice were resistant regardless of their genetic background. When we challenged mice with *S. typhimurium* by intraperitoneal injection, we noted no significant difference in the survival of *Tlr5*$^{+/+}$ and *Tlr5*$^{-/-}$ mice (**Fig. 7b**). Furthermore, we recovered fewer bacteria from the livers and spleens of *Tlr5*$^{-/-}$ mice than *Tlr5*$^{+/+}$ mice 4 d after oral infection (**Fig. 7c**). At 48 h after oral infection, *Tlr5*$^{+/+}$ and *Tlr5*$^{-/-}$ mice had the same number of *S. typhimurium* in Peyer's patches and LPCs. However, *Tlr5*$^{-/-}$ mice had fewer bacteria in MLNs than did *Tlr5*$^{+/+}$ mice (**Fig. 7d**). In addition, the proportion of *S. typhimurium*–laden CD11c$^+$ cells in MLNs of *Tlr5*$^{-/-}$ mice was smaller than that in *Tlr5*$^{+/+}$ mice (**Supplementary Fig. 3** online). To further determine whether the transport

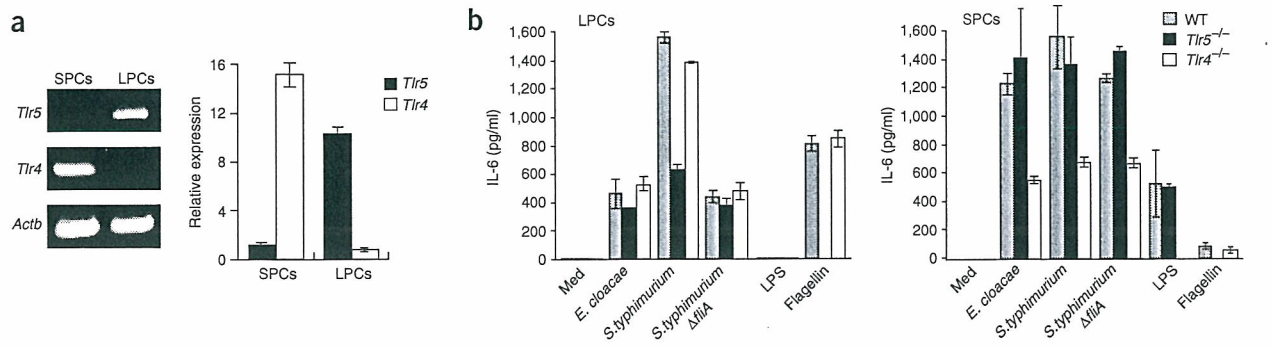


**Figure 6** CD11c$^+$ LPCs detect pathogenic bacteria via TLR5. (**a**) Quantitative real-time PCR of *Tlr5* and *Tlr4* expression in CD11c$^+$ SPCs and CD11c$^+$ LPCs of C57BL/6 mice. *Actb* encodes β-actin (loading control). Graphed data are mean ± s.d. of triplicate samples from one representative of three independent experiments. (**b**) Enzyme-linked immunosorbent assay of cytokine production by CD11c$^+$ SPCs and CD11c$^+$ LPCs from wild-type (WT), *Tlr4*$^{-/-}$ and *Tlr5*$^{-/-}$ mice, cultured with medium along (Med) or various stimuli (horizontal axes). Δ*fliA*, mutant strain lacking *fliA*. Data are mean ± s.d. of triplicate samples from one representative of three independent experiments.

of *S. typhimurium* from intestinal tract to MLNs was impaired in *Tlr5*$^{-/-}$ mice, we challenged *Tlr5*$^{+/+}$ and *Tlr5*$^{-/-}$ mice in a surgically isolated intestinal loop with *S. typhimurium* expressing green fluorescent protein (**Supplementary Fig. 4** online). We collected MLNs 24 h after infection. Staining showed that *Tlr5*$^{-/-}$ mice had fewer *S. typhimurium*–laden CD11c$^+$ cells (one to two cells per longitudinal slice of MLN) than did *Tlr5*$^{+/+}$ mice (about ten cells per longitudinal slice of MLN). Furthermore, no cells except CD11c$^+$ cells contained *S. typhimurium* in the infected MLNs. Thus, the impairment of transport of *S. typhimurium* from the intestinal tract to MLNs may lead to a delay in the establishment of systemic infection in *Tlr5*$^{-/-}$ mice.

## DISCUSSION

Although TLR5 has been identified as a receptor of flagellin *in vitro*, its *in vivo* function has remained unclear. Addressing the function of TLR5 in innate immunity has been difficult, because unlike other TLR family members, TLR5 is not expressed in mouse spleen cells, peritoneal macrophages or GM-DCs. Using a new method of isolating LPCs with high viability[9], we found that TLR5 is specifically expressed on CD11c$^+$ LPCs in mouse intestine. Although it has long been known that DCs are present in the lamina propria under the villus epithelium and take up antigens from the intestine[16], their functions and properties in the intestine were unknown. CD11c$^+$ LPCs elicited the secretion of various mediators, including inflammatory cytokines, chemokines, antimicrobial peptides and tissue remodeling kinases, in response to flagellin. Thus, we have shown here that immune responses are induced in CD11c$^+$ LPCs via TLR5.

Two points regarding the function of CD11c$^+$ LPCs in relation to TLR5 came to light as a result of our analyses. One was the cytokine profile of CD11c$^+$ LPCs stimulated with flagellin. The gut is continuously exposed to food antigens and many commensal bacteria. Tolerance to beneficial antigens seems to be controlled by mucosal DCs[17]. These DCs stimulate the activity of regulatory T cells, which are potent suppressors of T cell responses. A CD11c$^{lo}$CD45RB$^{hi}$ DC subset that produces IL-10 has been shown to specifically promote suppressive functions in regulatory T cells[14]. Peyer's patches contain DCs that produce IL-10 after inflammatory stimulation and thereby promote oral tolerance[12,13]. Whereas CD11c$^+$ PPCs induced IL-10 in response to LPS, flagellin-stimulated CD11c$^+$ LPCs did not produce IL-10, but instead produced IL-6 and IL-12, suggesting that CD11c$^+$ LPCs have a tendency to induce inflammatory responses rather than tolerance when stimulated with flagellin. However, it has been

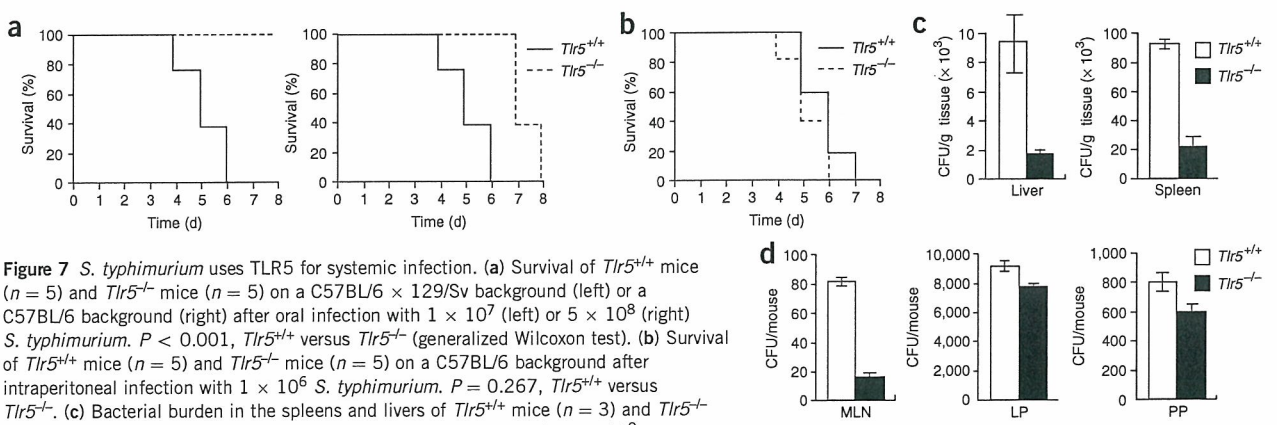


**Figure 7** *S. typhimurium* uses TLR5 for systemic infection. (**a**) Survival of *Tlr5*$^{+/+}$ mice ($n = 5$) and *Tlr5*$^{-/-}$ mice ($n = 5$) on a C57BL/6 × 129/Sv background (left) or a C57BL/6 background (right) after oral infection with $1 \times 10^7$ (left) or $5 \times 10^8$ (right) *S. typhimurium*. $P < 0.001$, *Tlr5*$^{+/+}$ versus *Tlr5*$^{-/-}$ (generalized Wilcoxon test). (**b**) Survival of *Tlr5*$^{+/+}$ mice ($n = 5$) and *Tlr5*$^{-/-}$ mice ($n = 5$) on a C57BL/6 background after intraperitoneal infection with $1 \times 10^6$ *S. typhimurium*. $P = 0.267$, *Tlr5*$^{+/+}$ versus *Tlr5*$^{-/-}$. (**c**) Bacterial burden in the spleens and livers of *Tlr5*$^{+/+}$ mice ($n = 3$) and *Tlr5*$^{-/-}$ mice ($n = 3$) on a C57BL/6 background 96 h after oral infection with $5 \times 10^8$ *S. typhimurium*. (**d**) Bacterial burden in the MLNs, PPCs and LPCs of *Tlr5*$^{+/+}$ mice ($n = 5$) and *Tlr5*$^{-/-}$ mice ($n = 5$) on C57BL/6 background 48 h after oral infection with $5 \times 10^8$ *S. typhimurium*. CFU, colony-forming units. Data are one representative of three independent experiments (**a**,**b**) or are mean ± s.d. of triplicate samples from one representative of three independent experiments (**c**,**d**).

reported that DCs in the lamina propria are involved in oral tolerance induction[18,19]. Further study will help elucidate CD11c$^+$ LPC-mediated regulation of tolerance and host defense.

The second notable point was that TLR4 expression was very low in CD11c$^+$ LPCs. Most commensal bacteria in intestine are Gram-negative anaerobic rod bacteria, which contain LPS in their cell wall. It has been shown that CD11c$^+$ LPCs extend their dendrites to sample bacteria in the intestinal lumen[20]. Although the mechanism of bacterial sampling by CD11c$^+$ LPCs was fully analyzed, it has remained unclear how host intestinal mucosa remains tolerant to commensal bacteria and discriminates between commensal and pathogenic bacteria. Low expression of TLR4 may allow CD11c$^+$ LPCs to avoid inducing inappropriate immune responses after exposure to commensal bacteria. Instead, CD11c$^+$ LPCs induced inflammatory responses after exposure to pathogenic flagellated bacteria mainly via TLR5. Some commensal bacteria also have flagella, but CD11c$^+$ LPCs did not respond vigorously to those bacteria. In addition, it has been reported that some commensal bacteria, such as α- and ε-proteobacteria, change the TLR5-recognition site of flagellin without losing flagellar motility[21]. Furthermore, some commensal bacteria suppress flagellin expression in stable host environments[12]. Therefore, unlike pathogenic bacteria, commensal bacteria may have mechanisms to escape TLR5-mediated host detection.

Other TLR family members, such as TLR2 and TLR4, also recognize bacterial components. The importance of TLR2 and TLR4 in host defense against various bacteria has been demonstrated with *Tlr2*$^{-/-}$ mice and *Tlr4*$^{-/-}$ mice. In particular, C3H/HeJ mice, which express a mutant form of TLR4, are highly susceptible to intraperitoneal infection by *S. typhimurium*[1]. Because TLR5 is highly expressed exclusively in the intestine, we predicted that no there would be no substantial difference in the survival of *Tlr5*$^{+/+}$ and *Tlr5*$^{-/-}$ mice after intraperitoneal infection. Instead, we predicted that disruption of *Tlr5* would render mice more susceptible to oral *S. typhimurium* infection, because stimulation of TLR5 induced the production of proinflammatory cytokines in CD11c$^+$ LPCs. The resistance of *Tlr5*$^{-/-}$ mice to oral *S. typhimurium* infection was unexpected. *Tlr5*$^{-/-}$ mice survived longer than *Tlr5*$^{+/+}$ mice because of impaired transport of *S. typhimurium* from the intestinal tract to the liver and spleen. We believe that this unexpected result is closely related to specific pathogenesis of salomonella. Most reports have indicated that *S. typhimurium* are captured by subepithelial DCs after transport through M cells in Peyer's patches[22] or by intraepithelial DCs that send protrusions into the lumen of the small intestine[23]. After being internalized, *S. typhimurium* actively modulates host vesicular trafficking pathways to avoid delivery to lysosomes and to establish a specialized replicative niche[24]. Bacteria-laden DCs undergo maturation and migrate to T cell zones of Peyer's patches or draining MLNs[12]. These mature DCs are also thought to be responsible for the dissemination of *S. typhimurium* through the bloodstream to the liver and spleen[12,25]. The uptake of *S. typhimurium* in Peyer's patches and LPCs was the same in *Tlr5*$^{+/+}$ and *Tlr5*$^{-/-}$ mice. Furthermore, the uptake of *S. typhimurium* was the same in *Tlr5*$^{+/+}$ and *Tlr5*$^{-/-}$ CD11c$^+$ LPCs *in vitro* (data not shown). However, there were many fewer bacteria in MLNs of *Tlr5*$^{-/-}$ mice than in *Tlr5*$^{+/+}$ mice, suggesting that the transport of *S. typhimurium* from lamina propria to MLNs was impaired. As *S. typhimurium* could not fully activate and mature *Tlr5*$^{-/-}$ CD11c$^+$ LPCs, migration of *S. typhimurium*–laden CD11c$^+$ LPCs from the periphery to circulation may be inefficient in *Tlr5*$^{-/-}$ mice. In support of that idea, there were many fewer *S. typhimurium*–laden CD11c$^+$ cells in *Tlr5*$^{-/-}$ mice than in *Tlr5*$^{+/+}$ mice after infection. Although TLR5 on CD11c$^+$ LPCs initially sense flagellated pathogenic bacteria to induce host defense, facultative intracellular pathogens such as *S. typhimurium* may use CD11c$^+$ LPCs as carriers for systemic infection. Further study will be needed to clarify the mechanism of systemic *S. typhimurium* infection, through the generation of a specific marker for CD11c$^+$ LPCs or a technique to specifically effect depletion of these cells. Finally, our work is likely to open new therapeutic perspectives. New methods that target TLR5 on CD11c$^+$ LPCs would be useful for mucosal adjuvant immune therapies.

## METHODS

**Mice, reagents and bacteria.** C57BL/6 mice were purchased from CLEA Japan. *Tlr4*$^{-/-}$ mice have been described[26]. *Tlr5*$^{-/-}$ mice are described in the **Supplementary Methods** online. All animal experiments were done with an experimental protocol approved by the Ethics Review Committee for Animal Experimentation of Research Institute for Microbial Diseases at Osaka University (Osaka, Japan). LPS from *Salmonella minnesota* Re595 was prepared with a phenol–chloroform–petroleum ether extraction procedure and purified flagellin was a gift from A. Aderem (Institute for Systems Biology, Seattle, Washington). *Salmonella enteritica* serovar typhimurium SR-11 x3181 and x3181 *fliA*::Tn*10* bacteria were provided by the Kitasato Institute for Life Science (Kitasato, Japan)[15,27]. *E. cloacae* was isolated from a healthy human volunteer and was identified by The Research Foundation for Microbial Diseases of Osaka University.

**Cells.** The preparation of GM-DCs and peritoneal macrophages has been described[28]. For the preparation of splenic macrophages and DCs, spleens were cut into small fragments and were incubated for 20 min at 37 °C with RPMI 1640 medium containing 400 U/ml of collagenase (Wako) and 15 μg/ml of DNase (Sigma). For the last 5 min, 5 mM EDTA was added. Single-cell suspensions were prepared after red blood cell lysis, and macrophages and DCs were positively selected with microbeads coated with antibody to CD11b (anti-CD11b) and anti-CD11 (Miltenyi), respectively. Intestinal lymphocytes and epithelial cells were isolated by a published protocol[9]. CD11c$^+$ cells from small intestine lamina propria and Peyer's patches were isolated by a published protocol[9].

**Measurement of proinflammatory cytokines.** GM-DCs, peritoneal macrophages, CD11b$^+$ splenocytes, CD11c$^+$ splenocytes and CD11c$^+$ LPCs were cultured in 96-well plates ($5 \times 10^4$ cells/well) with LPS (100 ng/ml) or flagellin (1 μg/ml). The concentrations of tumor necrosis factor, IL-6, IL-12p40 and IL-10 in culture supernatants were measured by the Bio-Plex system (Bio-Rad) following the manufacturer's instructions.

**PCR.** RNA (1 μg) was reverse-transcribed with Superscript2 (Invitrogen) according to the manufacturer's instructions with random hexamers as primers. PCR used the primer pairs in **Supplementary Table 1** online and Taq polymerase (Takara Shuzo). After being incubated at 95 °C for 10 min, products were amplified by 25 cycles of 97 °C (30 s), 57 °C (30 s) and 72 °C (30 s). Products were analyzed by agarose gel electrophoresis. Quantitative real-time PCR was done with a final volume of 25 μl containing cDNA amplified as described above, 2x PCR Master Mix (Applied Biosystems) and primers for 18S rRNA (Applied Biosystems) as an internal control or primers specific for *Tlr4* or *Tlr5* (Assay on Demand), using a 7700 Sequence Detector (Applied Biosystems). After being incubated at 95 °C for 10 min, products were amplified by 35 cycles of 95 °C (15 s), 60 °C (60 s) and 50 °C (120 s).

**Microarray analysis.** IECs and LPCs collected from *Tlr5*$^{+/+}$ and *Tlr5*$^{-/-}$ mice were left untreated or were treated for 4 h with flagellin (1 μg/ml). Total RNA was extracted with an RNeasy kit (Qiagen) and was purified with an Oligotex mRNA Kit (Pharmacia). Fragmented and biotin-labeled cDNA was synthesized from 100 ng purified mRNA with the Ovation Biotin System (Nugen) according to the manufacturer's protocol. The cDNA was hybridized to Affymetrix Murine Genome 430 2.0 microarray chips (Affymetrix) according to the manufacturer's instructions. Hybridized chips were stained and washed and were scanned with a GeneArray Scanner (Affymetrix). Microarray Suite software (Version 5.0, Affymetrix) and GeneSpring software (Silicon Genetics) were used for data analysis.

**Immunofluorescence.** Biotinylated monoclonal anti–mouse CD11c (HL3; Pharmingen) and anti-TLR5 (AP1505a; Abgent) were applied overnight at 4 °C to sections cut from frozen intestinal tissue. Samples were washed and then were incubated for 2 h at 25 °C with streptavidin–Alexa Fluor 594 (S-32356; Molecular Probes) and Alexa Fluor 488–chicken anti–rabbit IgG (A-21441; Molecular Probes). Staining was analyzed with a Radiance2100 laser-scanning confocal microscope (Bio-Rad). The intestinal loop assay is described in the **Supplementary Methods**.

**Bacterial infection.** *S. typhimurium* was grown in Luria-Bertani medium without shaking at 37 °C. The concentration of bacteria was determined by the absorbance at 600 nm. Bacteria were injected orally or intraperitoneally into 8-week-old mice. For determination of the bacterial burden in livers and spleens, LPCs, PPCs and MLNs were lysed with 0.01% Triton-X100. Serial dilutions of lysates were plated on Luria-Bertani agar plates and colonies were counted after overnight incubation at 37 °C.

**Statistics.** Kaplan-Meier plots and log-rank tests were used to assess the survival differences of control and mutant mice after bacterial infection.

**Accession code.** GEO: microarray data, GSE5119.

*Note: Supplementary information is available on the Nature Immunology website.*

ACKNOWLEDGMENTS

We thank K. Smith and T. Hawn (Institute for Systems Biology, Seattle, Washington) for providing purified flagellin; C. Sasagawa and T. Suzuki (Institute of Medical Science, Tokyo, Japan) for providing bacteria; members of the DNA-chip Development Center for Infectious Diseases (RIMD, Osaka University, Osaka, Japan) for technical advice; N. Kitagaki for technical assistance; and M. Hashimoto for secretarial assistance. Supported by Special Coordination Funds, the Ministry of Education, Culture, Sports, Science and Technology, and Research Fellowships of the Japan Society for the Promotion of Science for Young Scientists.

AUTHOR CONTRIBUTIONS

S.U. and M.H.J. did most of the experiments to characterize mouse phenotypes; N.C. helped with the quantitative PCR, microarray analysis, isolation of cells and enzyme-linked immunosorbent assays; Z.G. helped to isolate cells and with immunostaining and did the surgical operations for the intestinal loop assay; Y.K. helped with analysis of microarray data; M.Y. helped to generate *Tlr5*$^{-/-}$ mice; H.K. helped with the enzyme-linked immunosorbent assays; N.S. helped to isolate cells; H.M. provided *S. typhimurium* and provided instructions for infection experiments; H.K. helped with the infection experiments; H.H. helped to generate *Tlr5*$^{-/-}$ mice; C.C. helped with the infection experiments; T.K., K.J.I. and O.T. provided advice for the experiments; M.M. provided advice for the experiments and manuscript; K.T. helped to generate *Tlr5*$^{-/-}$ mice and to design experiments; and S.A. designed all the experiments and prepared the manuscript.

COMPETING INTERESTS STATEMENT

The authors declare that they have no competing financial interests.

Published online at http://www.nature.com/natureimmunology/
Reprints and permissions information is available online at http://npg.nature.com/reprintsandpermissions/

1. Akira, S., Uematsu, S. & Takeuchi, O. Pathogen recognition and innate immunity. *Cell* **124**, 783–801 (2006).
2. Hayashi, F. *et al.* The innate immune response to bacterial flagellin is mediated by Toll-like receptor 5. *Nature* **410**, 1099–1103 (2001).
3. Macnab, R.M. Genetics and biogenesis of bacterial flagella. *Annu. Rev. Genet.* **26**, 131–158 (1992).
4. Gewirtz, A.T., Navas, T.A., Lyons, S., Godowski, P.J. & Madara, J.L. Cutting edge: bacterial flagellin activates basolaterally expressed TLR5 to induce epithelial proinflammatory gene expression. *J. Immunol.* **167**, 1882–1885 (2001).
5. Salazar-Gonzalez, R.M. & McSorley, S.J. Salmonella flagellin, a microbial target of the innate and adaptive immune system. *Immunol. Lett.* **101**, 117–122 (2005).
6. Sierro, F. *et al.* Flagellin stimulation of intestinal epithelial cells triggers CCL20-mediated migration of dendritic cells. *Proc. Natl. Acad. Sci. USA* **98**, 13722–13727 (2001).
7. Sebastiani, G. *et al.* Cloning and characterization of the murine toll-like receptor 5 (*Tlr5*) gene: sequence and mRNA expression studies in Salmonella-susceptible MOLF/Ei mice. *Genomics* **64**, 230–240 (2000).
8. Hawn, T.R. *et al.* A common dominant TLR5 stop codon polymorphism abolishes flagellin signaling and is associated with susceptibility to legionnaires' disease. *J. Exp. Med.* **198**, 1563–1572 (2003).
9. Jang, M.H. *et al.* CCR7 is critically important for migration of dendritic cells in intestinal lamina propria to mesenteric lymph nodes. *J. Immunol.* **176**, 803–810 (2006).
10. Gewirtz, A.T. *et al.* Salmonella typhimurium translocates flagellin across intestinal epithelia, inducing a proinflammatory response. *J. Clin. Invest.* **107**, 99–109 (2001).
11. Pavli, P., Woodhams, C.E., Doe, W.F. & Hume, D.A. Isolation and characterization of antigen-presenting dendritic cells from the mouse intestinal lamina propria. *Immunology* **70**, 40–47 (1990).
12. Niedergang, F., Didierlaurent, A., Kraehenbuhl, J.P. & Sirard, J.C. Dendritic cells: the host Achille's heel for mucosal pathogens? *Trends Microbiol.* **12**, 79–88 (2004).
13. Ruedl, C., Rieser, C., Bock, G., Wick, G. & Wolf, H. Phenotypic and functional characterization of CD11c$^+$ dendritic cell population in mouse Peyer's patches. *Eur. J. Immunol.* **26**, 1801–1806 (1996).
14. Wakkach, A. *et al.* Characterization of dendritic cells that induce tolerance and T regulatory 1 cell differentiation in vivo. *Immunity* **18**, 605–617 (2003).
15. Kutsukake, K., Ohya, Y., Yamaguchi, S. & Iino, T. Operon structure of flagellar genes in Salmonella typhimurium. *Mol. Gen. Genet.* **214**, 11–15 (1988).
16. Mayrhofer, G., Pugh, C.W. & Barclay, A.N. The distribution, ontogeny and origin in the rat of Ia-positive cells with dendritic morphology and of Ia antigen in epithelia, with special reference to the intestine. *Eur. J. Immunol.* **13**, 112–122 (1983).
17. Mowat, A.M. Anatomical basis of tolerance and immunity to intestinal antigens. *Nat. Rev. Immunol.* **3**, 331–341 (2003).
18. Chirdo, F.G., Millington, O.R., Beacock-Sharp, H. & Mowat, A.M. Immunomodulatory dendritic cells in intestinal lamina propria. *Eur. J. Immunol.* **35**, 1831–1840 (2005).
19. Worbs, T. *et al.* Oral tolerance originates in the intestinal immune system and relies on antigen carriage by dendritic cells. *J. Exp. Med.* **203**, 519–527 (2006).
20. Niess, J.H. *et al.* CX3CR1-mediated dendritic cell access to the intestinal lumen and bacterial clearance. *Science* **307**, 254–258 (2005).
21. Andersen-Nissen, E. *et al.* Evasion of Toll-like receptor 5 by flagellated bacteria. *Proc. Natl. Acad. Sci. USA* **102**, 9247–9252 (2005).
22. Hopkins, S.A., Niedergang, F., Corthesy-Theulaz, I.E. & Kraehenbuhl, J.P. A recombinant Salmonella typhimurium vaccine strain is taken up and survives within murine Peyer's patch dendritic cells. *Cell. Microbiol.* **2**, 59–68 (2000).
23. Rescigno, M. *et al.* Dendritic cells express tight junction proteins and penetrate gut epithelial monolayers to sample bacteria. *Nat. Immunol.* **2**, 361–367 (2001).
24. Patel, J.C., Rossanese, O.W. & Galan, J.E. The functional interface between Salmonella and its host cell: opportunities for therapeutic intervention. *Trends Pharmacol. Sci.* **26**, 564–570 (2005).
25. Vazquez-Torres, A. *et al.* Extraintestinal dissemination of Salmonella by CD18-expressing phagocytes. *Nature* **401**, 804–808 (1999).
26. Hoshino, K. *et al.* Cutting edge: Toll-like receptor 4 (TLR4)-deficient mice are hyporesponsive to lipopolysaccharide: evidence for TLR4 as the Lps gene product. *J. Immunol.* **162**, 3749–3752 (1999).
27. Gulig, P.A. & Curtiss, R., III Plasmid-associated virulence of *Salmonella typhimurium*. *Infect. Immun.* **55**, 2891–2901 (1987).
28. Hemmi, H., Kaisho, T., Takeda, K. & Akira, S. The roles of Toll-like receptor 9, MyD88, and DNA-dependent protein kinase catalytic subunit in the effects of two distinct CpG DNAs on dendritic cell subsets. *J. Immunol.* **170**, 3059–3064 (2003).

nature immunology



# Key function for the Ubc13 E2 ubiquitin-conjugating enzyme in immune receptor signaling

Masahiro Yamamoto[1], Toru Okamoto[2], Kiyoshi Takeda[3], Shintaro Sato[4], Hideki Sanjo[1], Satoshi Uematsu[1], Tatsuya Saitoh[1,5], Naoki Yamamoto[5], Hiroaki Sakurai[6], Ken J Ishii[4], Shoji Yamaoka[5], Taro Kawai[4], Yoshiharu Matsuura[2], Osamu Takeuchi[1,4] & Shizuo Akira[1,4]

**The Ubc13 E2 ubiquitin-conjugating enzyme is key in the process of 'tagging' target proteins with lysine 63–linked polyubiquitin chains, which are essential for the transmission of immune receptor signals culminating in activation of the transcription factor NF-κB. Here we demonstrate that conditional ablation of Ubc13 resulted in defective B cell development and in impaired B cell and macrophage activation. In response to all tested stimuli except tumor necrosis factor, Ubc13-deficient cells showed almost normal NF-κB activation but considerably impaired activation of mitogen-activated protein kinase. Ubc13-induced activation of mitogen-activated protein kinase required, at least in part, ubiquitination of the adaptor protein IKKγ. These results show that Ubc13 is key in the mammalian immune response.**

Stimulation of Toll-like receptors (TLRs), interleukin 1 receptor (IL-1R), antigen receptors, CD40 and tumor necrosis factor receptor (TNFR) results in activation of mitogen-activated protein (MAP) kinases and of the transcription factor NF-κB. Such signals induce immune cell proliferation and survival and cytokine production[1]. In unstimulated cells, IκB proteins sequester NF-κB in the cytoplasm. Immune stimuli result in phosphorylation and ubiquitin- and proteasome-dependent degradation of IκB, thereby permitting translocation of NF-κB to the nucleus[2]. MAP kinases such as c-Jun N-terminal kinase (Jnk) and p38 are rapidly phosphorylated and activated by corresponding 'upstream' MAP kinase kinases, which are activated by MAP kinase kinase kinases. More than ten MAP kinase kinase kinases have been identified[3].

TLRs and IL-1R share 'downstream' signaling molecules, including MyD88, IL-1R-associated kinases (IRAKs) and TNFR-associated factor 6 (TRAF6)[4]. Genetic and biochemical studies suggest that TRAF6, the most distal of these shared signaling proteins, is pivotal in the TLR, IL-1R and CD40 signaling pathways[5]. Moreover, another TRAF family member, TRAF2, is required for TNFR signaling. These observations indicate the convergent function of the TRAF family members in innate immune signaling pathways[6]. Stimulation of B cell receptors (BCRs) and T cell receptors (TCRs) also activates NF-κB and MAP kinases[7]. Adaptor proteins such as Bcl-10, CARMA1 (also called CARD11 or Bimp3) and MALT1 (also called paracaspase) are required for BCR- and TCR-induced NF-κB and MAP kinase activation[8–14]. *In vitro* studies suggest that TRAF2 and TRAF6 are also involved in antigen receptor signaling[15].

TRAF2 and TRAF6 contain N-terminal RING finger domains that have E3 ubiquitin ligase activity[16]. Stimulus-dependent ubiquitination of TRAF6 activates the MAP kinase kinase kinase TGF-β-activated kinase (TAK1), which is critical in the activation of NF-κB and MAP kinases[17–19]. Moreover, TRAF6- and TRAF2-dependent ubiquitination of the adaptor protein IKKγ (also called NEMO) is involved in antigen receptor–induced NF-κB activation[15]. Polyubiquitin chains appended to TRAF and IKKγ are formed through linkages at lysine 63 (K63) of ubiquitin[20].

In contrast to lysine 48 (K48)–linked polyubiquitin chains, which induce proteasome-dependent degradation of the target proteins to which they are appended, K63-linked polyubiquitin chains have been linked to biological processes such as the stress response and DNA repair, rather than protein destruction[21]. K63-linked polyubiquitin chains are reportedly generated by the E2 ubiquitin-conjugating enzyme Ubc13 (ref. 22). The gene encoding Ubc13 was originally identified as being responsible for defective neural development in a drosophila mutant called *bendless*[23]. Subsequently, the synthesis of TRAF2- and TRAF6-dependent K63-linked polyubiquitin chains has been shown to be catalyzed by Ubc13 and Uev1A[16]. RNA silencing of the gene encoding Ubc13 results in defective NF-κB activation in HEK293 cells and insect cells[15,24–27], suggesting that the main function of Ubc13 is in NF-κB activation. In contrast, expression of dominant negative Ubc13 marginally affects TNF-induced NF-κB activation[28],

[1]Department of Host Defense and [2]Department of Molecular Virology, Research Institute for Microbial Diseases, Osaka University, Osaka 565-0871, Japan. [3]Department of Embryonic and Genetic Engineering, Medical Institute of Bioregulation, Kyushu University, Fukuoka 812-8582, Japan. [4]ERATO, Japan Science and Technology Corporation, Osaka 565-0871, Japan. [5]Department of Molecular Virology, Graduate School of Medicine, Tokyo Medical and Dental University, Tokyo 113-8519, Japan. [6]Division of Pathogenic Biochemistry, Institute of Natural Medicine, 21st Century Center of Excellence Program, Toyama Medical and Pharmaceutical University, Toyama 930-0194, Japan. Correspondence should be addressed to Shizuo Akira (sakira@biken.osaka-u.ac.jp).

Received 21 February; accepted 29 June; published online 23 July 2006; doi:10.1038/ni1367

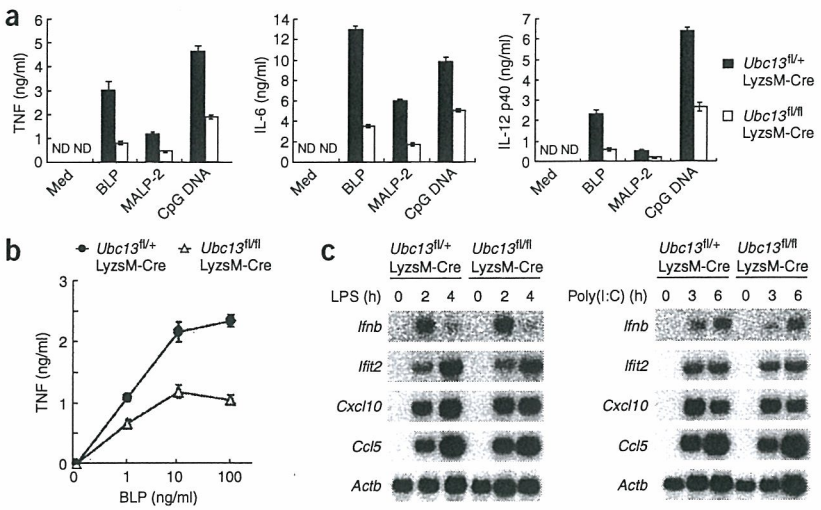


**Figure 1** Defective proinflammatory cytokine production in Ubc13-deficient bone marrow macrophages. (**a**) ELISA of IL-6, TNF and IL-12p40 in culture supernatants of bone marrow macrophages (mouse genotypes, key) cultured for 24 h with 100 ng/ml of BLP, 30 ng/ml of MALP-2 or 1 μM CpG DNA in the presence of 30 ng/ml of interferon-γ. Med, medium only; ND, not detected. (**b**) ELISA of TNF in culture supernatants of bone marrow macrophages (mouse genotypes, key) cultured for 24 h with BLP (concentration, horizontal axis) in the presence of 30 ng/ml of interferon-γ. Data (**a**,**b**) represent mean ± s.d. of triplicate samples and are representative of three independent experiments. (**c**) RNA blot analysis of total RNA (10 μg) extracted from bone marrow macrophages (mouse genotypes, above blots) stimulated with 100 ng/ml of LPS (left) or 50 μg/ml of poly(I:C) (right). *Ifnb*, *Ifit2*, *Cxcl10*, *Ccl5* and *Actb* encode interferon-β, ISG54, IP-10, RANTES and β-actin, respectively. Data are representative of two independent experiments.



and the RING finger domain of TRAF6, which is essential for ligation of K63-linked polyubiquitin chains to target proteins, is dispensable for the IL-1R- and TLR-mediated NF-κB activation[29]. Those results suggest that Ubc13 has a minor function in NF-κB activation. Thus, whether Ubc13 is essential for immune signaling and immune responses *in vivo* is not known.

Here we have generated mice conditionally deficient in Ubc13. We demonstrate that Ubc13 was essential for TLR-induced proinflammatory cytokine production in bone marrow–derived macrophages. In addition, Ubc13 was required for TLR-, CD40- and BCR-induced B cell activation. B cell–specific deletion of Ubc13 resulted in defective development of marginal zone B cells and B-1 cells and in impaired humoral immune responses. Ubc13-deficient cells had almost normal NF-κB activation and normal TAK1 phosphorylation. In contrast, Ubc13-deficient cells had substantially impaired MAP kinase activation in response to all stimuli tested, except for TNF. Ubc13-induced MAP kinase activation was mediated partially through ubiquitination of IKKγ, which was abolished in Ubc13-deficient cells. Our results demonstrate the physiological importance of Ubc13 in the induction of mammalian immune responses.

## RESULTS

### Conditional ablation of Ubc13

To assess the function of Ubc13 in adult mice, we generated mice in which Ubc13 could be conditionally ablated (**Supplementary Fig. 1** online). The gene encoding Ubc13 (called '*Ubc13*' here) consists of four exons. We constructed a targeting vector to insert *lox*P sites flanking exons 2, 3 and 4 of *Ubc13* and to insert a *lox*P-flanked neomycin-resistance gene into intron 1 of *Ubc13*. To generate conventional Ubc13-deficient ($Ubc13^{-/-}$) mice, we constructed another targeting vector lacking the flanked exons (data not shown). In both cases, we microinjected two correctly targeted embryonic stem cell clones into C57BL/6 blastocysts to generate chimeric mice. We crossed male chimeric with female C57BL/6 mice and monitored transmission of the mutated allele by Southern blot analysis (**Supplementary Fig. 1** and data not shown). Although $Ubc13^{+/-}$ mice were phenotypically normal and fertile, we failed to obtain $Ubc13^{-/-}$ offspring by intercrossing $Ubc13^{+/-}$ mice (**Supplementary Table 1** online). To determine the time of death *in utero*, we genotyped embryos from $Ubc13^{+/-}$ intercrosses at embryonic day 13.5 or 9.5. We detected no $Ubc13^{-/-}$ embryos, indicating that Ubc13 deficiency results in early embryonic death. In contrast, mice homozygous for *lox*P-flanked *Ubc13* alleles ($Ubc13^{fl/fl}$ mice) were born at the expected mendelian ratios and had no obvious abnormalities (data not shown).

### Ubc13 in macrophage activation

Because Ubc13 has been linked to the activation of TRAF6, a crucial component of TLR signaling pathways[16,30], we assessed the function of Ubc13 in the TLR responses in bone marrow–derived macrophages. To disrupt *Ubc13* specifically in macrophages, were crossed $Ubc13^{fl/fl}$ mice with mice in which cDNA encoding Cre recombinase is inserted into the gene encoding lysozyme M, which is specifically expressed in the myeloid linage such as macrophages and granulocytes (LyzsM-Cre mice). Southern blot analysis showed that in bone marrow macrophages from the resultant '$Ubc13^{fl/fl}$LyzsM-Cre mice', Cre-mediated deletion produced a new 1.1-kb band corresponding to the mutated *Ubc13* allele, and immunoblot analysis showed that $Ubc13^{fl/fl}$LyzsM-Cre bone marrow macrophages had much less Ubc13 protein than did control cells (**Supplementary Fig. 1**).

Bone marrow macrophages produce proinflammatory cytokines in response to a variety of TLR ligands in a MyD88-dependent way[4]. Thus, we assessed cytokine production by $Ubc13^{fl/fl}$LyzsM-Cre bone marrow macrophages stimulated with TLR ligands such as BLP, MALP-2 and CpG DNA. Bone marrow macrophages from $Ubc13^{fl/fl}$LyzsM-Cre mice produced less TNF, IL-6 and IL-12p40 than did those from control mice (**Fig. 1a**), and the response to BLP was dose dependent (**Fig. 1b**). These results indicate that Ubc13 is important in TLR-induced cytokine production in bone marrow macrophages.

TLR signaling can be MyD88 dependent or MyD88 independent. MyD88-independent TLR3 and TLR4 signaling results in the induction of type I interferon and interferon-inducible genes[4]. To assess the function of Ubc13 in MyD88-independent immune responses, we analyzed expression of the gene encoding interferon-β and of interferon-inducible genes, including *Ifit2*, *Cxcl10* and *Ccl5*, after treatment of control or $Ubc13^{fl/fl}$LyzsM-Cre bone marrow macrophages with lipopolysaccharide (LPS) or poly(I:C). Control and $Ubc13^{fl/fl}$LyzsM-Cre bone marrow macrophages contained similar amounts of transcripts encoding interferon and of interferon-inducible gene transcripts after LPS or poly(I:C) stimulation, indicating that

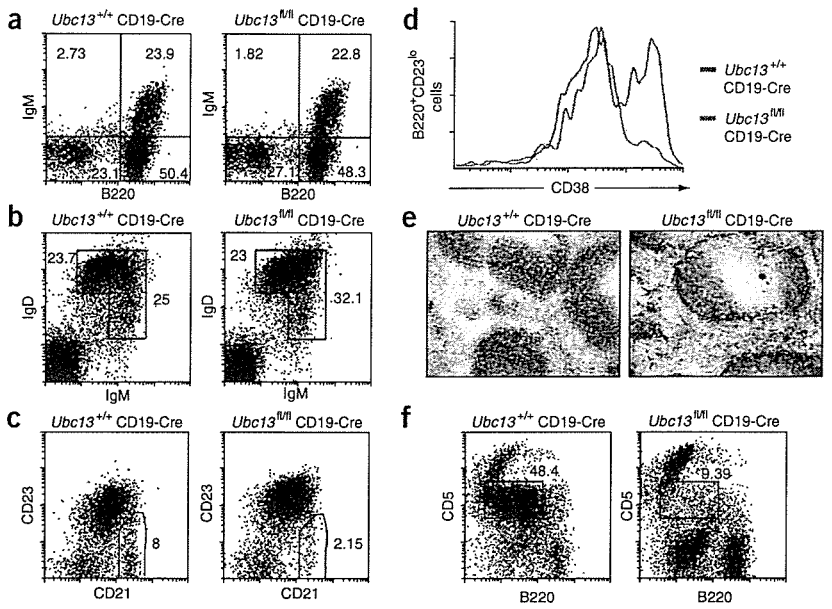


**Figure 2** Impaired B cell development in *Ubc13*$^{fl/fl}$Cd19-Cre mice. (**a–d**) Flow cytometry of IgM and B220 expression by B cell precursors in the bone marrow (**a**) and of IgM and IgD expression (**b**), CD21 and CD23 expression by B220$^+$ populations (**c**) and CD38 expression by B220$^+$CD23$^{lo}$ populations (**d**) of B cells in the spleens of 6- to 10-week-old mice. (**e**) Frozen splenic sections stained with rat monoclonal antibody to mouse metallophilic macrophages (red) and with anti-B220 to visualize B cells (blue). Original magnification, ×200. (**f**) Flow cytometry of B220 and CD5 expression by CD5$^+$ B cells in the peritonea of 6- to 10-week-old mice. Numbers in dot plots indicate percentages of cells in each quadrant (**a**); of mature (**b**, left) and immature (**b**, right) splenic B cells; of marginal zone B cells (**c**); and of B1 cells (**f**). Data are representative of three independent experiments.

Ubc13 is dispensable for the TLR-mediated MyD88-independent immune responses in bone marrow macrophages (**Fig. 1c**).

## Ubc13 in B cell development and function

Mice lacking molecules involved in BCR signaling show defective B cell development. Specifically, mice lacking the Bcl-10 or MALT1 adaptor proteins show defective development of marginal zone B cells and B-1 B cells[9,13,31]. The adaptor protein CARMA1 is also essential for the generation of B-1 B cells[10–12,14]. To determine whether Ubc13 deficiency affects the B cell development, we generated mice lacking Ubc13 specifically in the B cell lineage. We crossed *Ubc13*$^{fl/fl}$ mice with mice expressing a Cre transgene under control of the *Cd19* promoter (Cd19-Cre mice). Southern blot and immunoblot analysis showed almost complete Cre-mediated deletion of the *Ubc13 lox*P-flanked alleles and the protein in splenic B220$^+$ cells from these '*Ubc13*$^{fl/fl}$ Cd19-Cre mice' (**Supplementary Fig. 1**).

To determine whether the Ubc13 disruption affected B cell development, we examined the bone marrow of control and *Ubc13*$^{fl/fl}$Cd19-Cre mice. Control and *Ubc13*$^{fl/fl}$Cd19-Cre mice had no differences in bone marrow cellularity, and B cell precursor populations in control and *Ubc13*$^{fl/fl}$Cd19-Cre mice had similar expression of surface B220 and immunoglobulin M (IgM; **Fig. 2a**). Moreover, splenocytes from *Ubc13*$^{fl/fl}$Cd19-Cre mice had a pattern of surface expression of CD3 and B220 similar to that of control mice (**Supplementary Fig. 2** online). Whereas the expression of IgM and IgD was similar on the surfaces of splenocytes from control and *Ubc13*$^{fl/fl}$Cd19-Cre mice (**Fig. 2b**), *Ubc13*$^{fl/fl}$Cd19-Cre mice had a much lower frequency of B220$^+$CD21$^{hi}$CD23$^{lo}$ marginal zone B cells (**Fig. 2c**). Detection of marginal zone B cells with another set of surface antigens, B220, CD38 and CD21, produced similar results (**Fig. 2d**). Immunohistochemical staining confirmed that the width of marginal zone B cell area was smaller in spleens from *Ubc13*$^{fl/fl}$Cd19-Cre mice (**Fig. 2e**). The CD5$^+$ peritoneal B-1 cell population was also much lower in *Ubc13*$^{fl/fl}$Cd19-Cre mice (**Fig. 2f**). These results suggest that Ubc13 is essential for the development of marginal zone B cells and peritoneal CD5$^+$ B-1 cells.

To test whether Ubc13 is involved in TLR responses in B cells, we analyzed the proliferation of control and *Ubc13*$^{fl/fl}$Cd19-Cre B cells stimulated with LPS or CpG DNA. Control B cells proliferated in a dose-dependent way in response to both LPS and CpG DNA stimulation (**Fig. 3a**). In contrast, proliferation of *Ubc13*$^{fl/fl}$Cd19-Cre B cells in response to these stimuli was much lower. In addition, CpG DNA–induced IL-6 production in *Ubc13*$^{fl/fl}$Cd19-Cre B cells was severely impaired (**Fig. 3b**). Compared with control B cells, *Ubc13*$^{fl/fl}$Cd19-Cre B cells also showed defective proliferation in response to stimulation with antibody to IgM (anti-IgM) or anti-CD40 (**Fig. 3a**). We next assessed whether these defects in TLR-, BCR- and CD40-mediated proliferation were accompanied by impaired cell cycle progression in *Ubc13*$^{fl/fl}$Cd19-Cre B cells. Compared with control B cells, which entered S phase after stimulation with LPS, CpG DNA, anti-IgM or anti-CD40, fewer *Ubc13*$^{fl/fl}$Cd19-Cre B cells entered S phase after stimulation (**Fig. 3c**). Stimulation with LPS, CpG DNA or anti-CD40 can prevent B cell apoptosis that normally results from *ex vivo* culture of B cells without mitogens[19]. A greater proportion of *Ubc13*$^{fl/fl}$Cd19-Cre B cells than control B cells underwent apoptosis *ex vivo*, even after stimulation with LPS, CpG DNA or anti-CD40 (**Fig. 3d**). These results collectively suggest that Ubc13 is critical for TLR-, BCR-, and CD40-mediated B cell activation, proliferation and survival.

To investigate whether the defective activation and development of *Ubc13*$^{fl/fl}$Cd19-Cre B cells affected on the immune responses *in vivo*, we compared immunoglobulin concentrations in sera of control and *Ubc13*$^{fl/fl}$Cd19-Cre mice (**Fig. 3e**). All immunoglobulin isotypes tested except IgG2a and IgG2b were significantly lower in *Ubc13*$^{fl/fl}$ Cd19-Cre mice than in control mice. After immunization with the T cell–independent polyvalent antigen trinitrophenol-Ficoll or the T cell–dependent antigen nitrophenol–chicken γ-globulin, *Ubc13*$^{fl/fl}$ Cd19-Cre mice had significantly less serum trinitrophenol-specific IgM and IgG3 (**Fig. 3f**). Although nitrophenol-specific IgM titers were similar, nitrophenol-specific IgG1 titers were lower in *Ubc13*$^{fl/fl}$Cd19-Cre mice (**Fig. 3g**). Thus, Ubc13 is required for appropriate humoral immune responses *in vivo*.

## Ubc13 in NF-κB and MAPK activation

TLR, BCR, CD40, IL-1R and TNFR signals culminate in NF-κB activation[32]. Although *in vitro* studies indicate that Ubc13 is involved in NF-κB activation in HEK293 cells[33], whether Ubc13 deficiency affects NF-κB activation mediated by TLR, BCR, CD40, TNFR or IL-1R in other cell types in physiological conditions is not known.